



A minerals research contract report
FEBRUARY 1986

ON THE DEVELOPMENT OF A MODEL-BASED CONTROL STRATEGY FOR COPPER-ORE FLOTATION

OFR 86-38

Contract J0215035
University of Utah

**BUREAU OF MINES
UNITED STATES DEPARTMENT OF THE INTERIOR**

OFR
86-38



The views and conclusions contained in this document are those of the authors and should not be interpreted as necessarily representing the official policies or recommendations of the Interior Department's Bureau of Mines or of the U.S. Government.

FOREWORD ***

This report was prepared by the Department of Metallurgy and Metallurgical Engineering of University of Utah, under USBM Contract number J0215035. This contract was initiated under the Minerals and Materials Research Program. This project was administered under the technical direction of Dr. John A. Herbst of the University of Utah with the support of Dr. Roberto Zaragoza and Dr. Osvaldo A. Bascur. Dr. Stephen D. Hill, Director, Salt Lake City Research Center, was the Technical Project Officer for the Bureau of Mines. This report is a summary of the work recently completed under the subject contract during the period July 1, 1981 to March 31, 1985. This report was originally submitted by the authors in February of 1985. Recommendations and criticisms were made by USBM personnel and are reflected in this final report.

CONTENTS

	<u>Page</u>
Foreword.....	4
List of Illustrations.....	6
List of Tables.....	7
Abstract.....	8
Introduction.....	8
Model-based alternative.....	12
Model development.....	13
Particle flotation model.....	20
Rate constants in particle balances.....	22
Attachment phenomena in the pulp.....	22
Detachment phenomena in the pulp.....	24
Attachment phenomena in the froth.....	25
Detachment phenomena in the froth.....	26
Water Model.....	29
Water entrainment.....	29
Water drainage.....	31
Water into the concentrate.....	33
Model parameterization.....	34
Experimental procedure.....	34
Dynamic Simulator.....	38
Simulator development.....	38
Simulator verification.....	42
Simplified model and verification.....	42
Description of control strategies.....	48
Implementation of a Kalman filter.....	48

Control strategies.....	50
Grade of chalcopyrite controller.....	54
Recovery of chalcopyrite controller.....	54
On-line sensing of ore characteristics.....	57
Control objectives.....	59
Grade-recovery map.....	60
On-line adjustment of the mass balance.....	62
Conclusions.....	62
References.....	64

ILLUSTRATIONS

1. Schematic representations of a model-based control strategy....	14
2. Schematic representation of a flotation cell.....	18
3. Four states for particles in a flotation cell.....	19
4. Schematic of pilot circuit.....	35
5. Experimental and simulated concentrations of chalcopyrite in concentrate and tailing by size.....	39
6. DYNAFLOAT program flowchart.....	40
7. Dynamic verification of the model for aeration, frother step changes, and feed disturbances under level control.....	43
8. Simplified model dynamic verification.....	47
9. Estimation of concentrate grade and recovery of copper from measurements of tailing percent copper using a Kalman Filter...	51
10. Simulated grade-air and grade-level control loop responses of recovery and grade.....	55
11. Simulated recovery-air and recovery-level control loop responses of recovery and grade.....	56

12.	On-line estimation of ore changes and mass balancing for a copper sulfide flotation circuit.....	58
13.	Grade-recovery map provided by the adaptive phenomenological flotation model in the pilot plant.....	61

TABLES

1.	Variables of importance for flotation of sulfide copper ores...	11
2.	Population balance model for four states in a flotation cell...	22
3.	Typical steady-state adjusted data.....	37
4.	Comparison of simplified model with experimental data for steady-state copper sulfide ore, experiment B-3.....	46
5.	Response of controlled variables to changes in some manipulated variables as indicated by the process matrix.....	53

ON THE DEVELOPMENT OF A MODEL-BASED
CONTROL STRATEGY FOR COPPER-ORE FLOTATION

J. A. Herbst,¹ R. Zaragoza,² and O. A. Bascur³

*** ABSTRACT

During the last decade it has been established that conventional flotation control strategies based on classical control theory result in significant increases in grade, recovery, and operating-cost savings. In the current report a description of an advanced model-based control philosophy is presented. The derivation and verification of a simplified flotation model is described. The implementation of a Kalman filter for estimation of unmeasured variables for input to controllers is discussed. Several control strategies using the model-based approach are described, emphasizing the nonlinear nature of the flotation plant. Expected trends in the implementation of such model-based flotation control strategies in the future are discussed.

*** INTRODUCTION

The research presented in this report was carried out under the sponsorship of Contract No. JO 215035. This research was initiated because it has been perceived by academics, the government, and minerals industry users that the development of a model-based control strategy for flotation has considerable economic potential with expected payoffs in the range of 5-10% increase in throughput, with higher recoveries and

¹Professor

²Graduate Student

³Former Graduate Student*

Department of Metallurgy and Metallurgical Engineering, University of Utah, Salt Lake City, Utah.

*Currently research engineer, Duval Corporation, Tucson, Arizona.

higher product grades. The first step in the development of such strategies involves the construction of an accurate dynamic model for the flotation process. This research has concentrated on the development of such a model and has looked toward the use of this model in copper-ore flotation control strategies.

The use of process computers combined with on-line x-ray fluorescence (XRF) in industrial flotation circuits has made the application of more sophisticated control techniques feasible in the mineral-recovery process. In spite of the availability of good instrumentation in modern flotation plants, current control strategies are far less effective than they should be. Classical control methods in use today have some important limitations for control of flotation plants. A major limitation results from the fact that single-input/single-output control-loop linkings can result in highly undesirable interactions between controllers. An example of such interactions is a flotation-control strategy in which aeration rate is manipulated to control the grade of the froth product while pulp level is manipulated to control mineral recovery (1,2).⁴ In this case the manipulation of the aeration rate affects not only the grade but also the recovery. Similarly, the manipulation of the pulp level to control the recovery affects not only the recovery (the variable it is linked to through the controller) but also the grade. Under such conditions, if the grade is below the setpoint value and the recovery is too low, the grade controller will work against the recovery controller since a reduction in the aeration

⁴Underlined numbers in parentheses refer to items in the list of references at the end of this report.

to increase the grade will simultaneously reduce the recovery. In practice, instabilities arising from the interaction of controllers are usually minimized by detuning of one or more loops. Detuning of loops results in a general slow-down in control response, which is inconsistent with the control objective of achieving a rapid response to circuit perturbation in order to maintain optimum operation.

Many of the limitations in classical control strategies discussed above are due to a lack of information about the magnitude of control-variable responses to changes in the manipulated variables and the nature of the interactions between variables. The problem is further aggravated by the non-linear nature of the flotation process and the signals corrupted with noise obtained from sensors.

Important factors such as changes in the ore type and water chemistry are always present. Several of these changes are either difficult or impossible to measure on-line, including variables such as liberation characteristics, ore specific gravity, pulp chemistry, slurry viscosity, soluble salts in the ore, froth stability, and flotability. In addition, changes in equipment (e.g., wear) can cause a gradual drift in the dynamic performance of the process. A complete list of variables of importance in flotation of minerals is given in table 1. Because most current control systems can not adapt specifically to such fluctuations, their performance is suboptimal.

TABLE 1. - Variables of importance for flotation of minerals

<u>DISTURBANCE</u>		<u>CONTROLLED</u>
Mineralogical Composition		Recovery (product tonnage)
Uncontrolled Feedrate		Grade
Uncontrolled Feed Size		Circulating Loads
Liberation State		Froth Levels
Fluctuating Head Grades		Percent Solids
Surface Modifications		
Water Composition		
<u>MANIPULATED</u>		<u>MEASURED</u>
<u>Physical</u>	<u>Chemical</u>	Assays
Aeration	Frothers	Volume Flowrate
Pulp Levels	Reagents (collectors,	Pulp Densities
Impeller Speed	depressants,	
Conditioning Time	activators, pH)	
Froth Removal	Addition Points	

Another very important consideration in the control of flotation circuits is that not all streams can be sampled, either for economic or technical reasons. In practice the frequency of invalid information may be large; for example, in the flotation feed stream, fluctuations in grinding may produce coarse particles which result in problems in the sampling system. When head or tail assay streams yield invalid information, the control system needs to respond in a satisfactory manner for stable operation. Several material balance calculations to adjust steady-state data can be used to partially solve these problems (3). Calculations of recoveries using XRF during circuit upsets using traditional formulas can be inaccurate. For good control, the unsteady-state disturbance period is precisely when good filtered grade and recovery estimates are most critical.

During the last few years new and promising approaches to solving some

of these problems have emerged (1,4,5). These approaches are based on the use of an on-line dynamic model of the flotation process to make predictions which are useful for control decision-making. These predictions are based on a logical compromise among instrument readings, the on-line model, and good engineering judgement.

This report presents developments in model-based control as applied to the flotation of a copper sulfide ore. The development and verification of an on-line model for sulfide flotation are presented, and the use of the model for obtaining unmeasured states necessary for control action is discussed. Several implications of the model-based control philosophy are presented.

*** ACKNOWLEDGEMENTS

The authors wish to thank Mr. Lynn Hales of Kennecott Copper Corporation for supplying the tonnage samples used in pilot-scale tests and Mr. Don Foot Group Supervisor of the US Bureau of Mines Salt Lake City Research Center for arranging for the crushing of these samples. Helpful discussions on control strategies with Mr. Hales and Dr. Steve Hill, Research Director, US Bureau of Mines Salt Lake City Research Center are also gratefully acknowledged.

*** MODEL-BASED ALTERNATIVE

A classical feedback control method assumes that the direction of change in a manipulated variable required for correction of a control variable is known and that a set of controller gains can be found that is suitable for all circumstances. It is easily recognized that for flotation of sulfide minerals no unique set of tuning constants for such a simple description is available in most cases, and that some form of control strategy adaptation to disturbance is desirable.

A promising solution to such a problem involves building a model that contains the missing information about the flotation process. By incorporating an on-line flotation model in the control strategy, well-informed responses to disturbances can be made, and an "optimal" control performance can ultimately be achieved. An adjusted dynamic on-line mass balance of the flotation plant is obtained from which several control alternatives can be visualized.

The nature of the model-based control strategy for a flotation operation is revealed in figure 1 (1). The essential features are as follows:

- 1) a process model that is simple enough to be used for rapid on-line calculation but detailed enough to faithfully reproduce the essential dynamic characteristics of the process,
- 2) an estimator that combines process measurements and model information to obtain best estimates of the "state of the system" and parameters of the process at any instant of time,
- 3) an optimizer that uses the current state of the system and the model to select the path for manipulated variables which will result in achieving process objectives in an optimal way. In such a scheme, the optimizer supervises the setpoints of standard regulatory control loops and provides the optimal trajectories to the controllers,
- 4) a controller that accepts setpoint values and/or control loop gains specified by the optimizer.

The control-system structure (fig. 1) allows the controller to adapt to plant disturbances and/or to accommodate changes in management operating policies. Adaptation is achieved using a model and an

MODEL BASED SUPERVISORY CONTROL

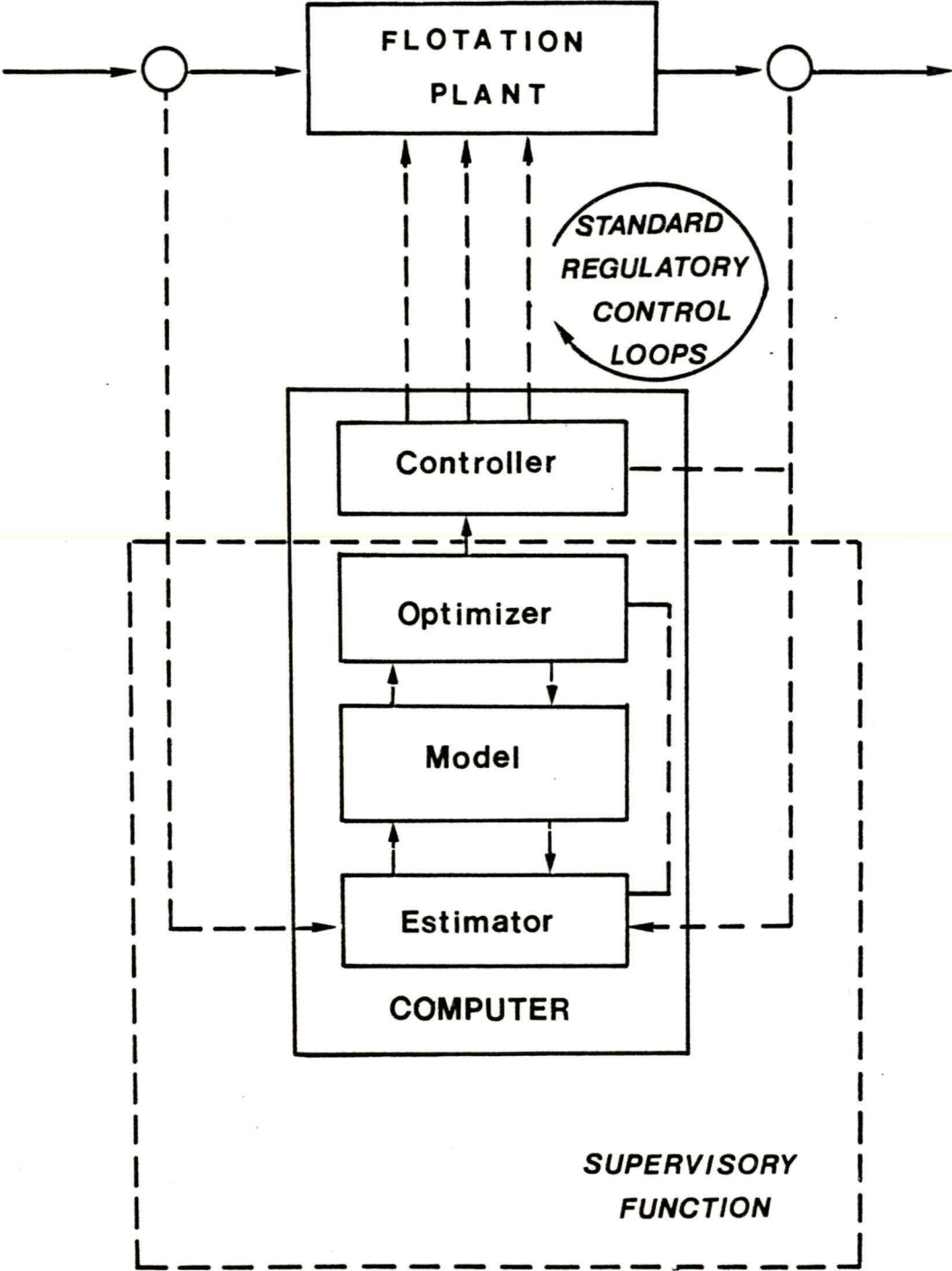


Figure 1. Schematic representation of a model-based control strategy.

estimator utilizing feedback from measurements of the process input and output signals. Based on this information the best controller output can be calculated.

The following sections contain: 1) the general model development, 2) the model parameterization and experimental set-up, 3) a brief description of the general simulation and its verification, 4) a description of a simplified flotation model, 5) the implementation of a Kalman Filter for estimation of unmeasured variables for input to controllers, and 6) the implications of these models for control.

*** MODEL DEVELOPMENT

The two major classes of process models for control are the phenomenological models, derived from conservation of mass, momentum, and energy equations, and the empirical models that use general input-output relationships obtained from stimulus-response experiments. The phenomenological models require knowledge of the physics and chemistry of the important subprocesses and their behavior, while the empirical models do not require such knowledge. An empirical (black-box) model can be developed fairly quickly due to its simplicity, but this simplicity usually leads to a model which is only valid over narrow operating conditions. Since mineral-processing plants are often subject to large process upsets this latter approach is severely limited in its applicability.

In contrast to empirical models, the phenomenological models (which obtain their form from theory) are usually valid over a wide range of operating conditions. A drawback associated with the phenomenological approach is that the necessary physical knowledge required for the model is not always available. These models tend to be complex, and they

often take a great deal of time to develop. Ultimately, however, only the phenomenological models can be extrapolated beyond the particular conditions under which data were gathered.

The approach adopted for developing a dynamic model of flotation-cell performance is one in which the physics and chemistry of this complex process are reflected in the equations to the maximum degree they have been described in the literature. In many ways the development parallels that given by Mika and Fuerstenau (10); however, in the current work the emphasis is on making the model useful for automatic control applications. In this regard, care has been taken to include as many process upsets, manipulated, and control variables in the model equations as possible. Further, the model is formulated in such a way that all model constants can be evaluated readily from experimental data.

The manipulated variables of any flotation process can be divided into two groups, physical and chemical. The physical-variable category includes impeller speed, aeration rate, pulp level, froth removal rate and others. The chemical-variable category includes addition rates of collector, frother, depressant, modifier, conditioning times, etc. A complete list of manipulated and controlled variables for flotation is given in table 1.

In the development of the model which follows, an attempt has been made to include all of the physical, manipulated variables and all possible controlled and measured variables. For the purpose of model development, an abstraction of the process is made as shown in figure 2. The flotation process involves the interaction of three phases, solid, liquid and gas. The flotation cell is divided in two volumes,

the pulp zone in which intimate particle-bubble contact is induced by the turbulent action of the impeller and the froth zone which acts as a separating medium to segregate and to remove the valuable minerals.

The pulp zone and the froth zone are subdivided in the liquid and air phases, and associated with each of these phases are the particles undergoing separation. V_{LP} and V_{LF} are defined as the unaerated liquid volumes, and V_{BP} and V_{BF} are volumes of the air phase in the pulp and in the froth zones respectively.

In practice there are a variety of mechanisms whereby a particle can be transported from the pulp into the froth, i.e., by levitation on air bubbles, by water entrainment, or by slime attachment to other particles. In addition, particles can drain back into the pulp volume or leave the froth zone by entering the concentrate launder. These mechanisms are all shown schematically in figure 3.

In this development, it will be assumed that the pulp zone is well mixed. A number of experimental studies have proven this to be a good approximation. This assumption has been critically reviewed by Lynch (11) and more recently by Mehotra and Saxena (12). The assumption of good mixing does not apply to the froth volume, which, strictly speaking, should be regarded as horizontally homogeneous and distributed in height. In treating the distributed nature of the froth, in some instances it has been considered as a plug flow process (13), and in others it has been subdivided into one or more zones (14-16). The investigators who consider the behavior of the air and liquid phases separately are Mika and Fuerstenau (10), Moys (13), and Flint (17). This approach is vital for explaining the cleaning action of the froth.

Despite the greater intuitive appeal of the distributed parameter

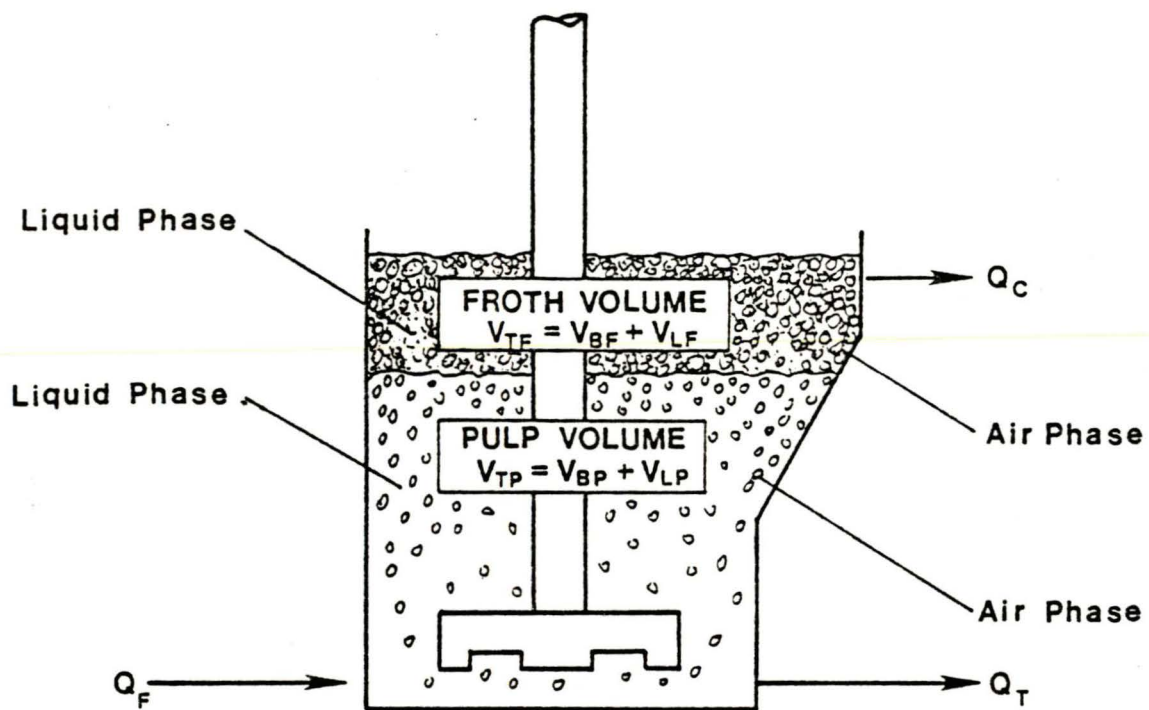


Figure 2. Schematic representation of a flotation cell.

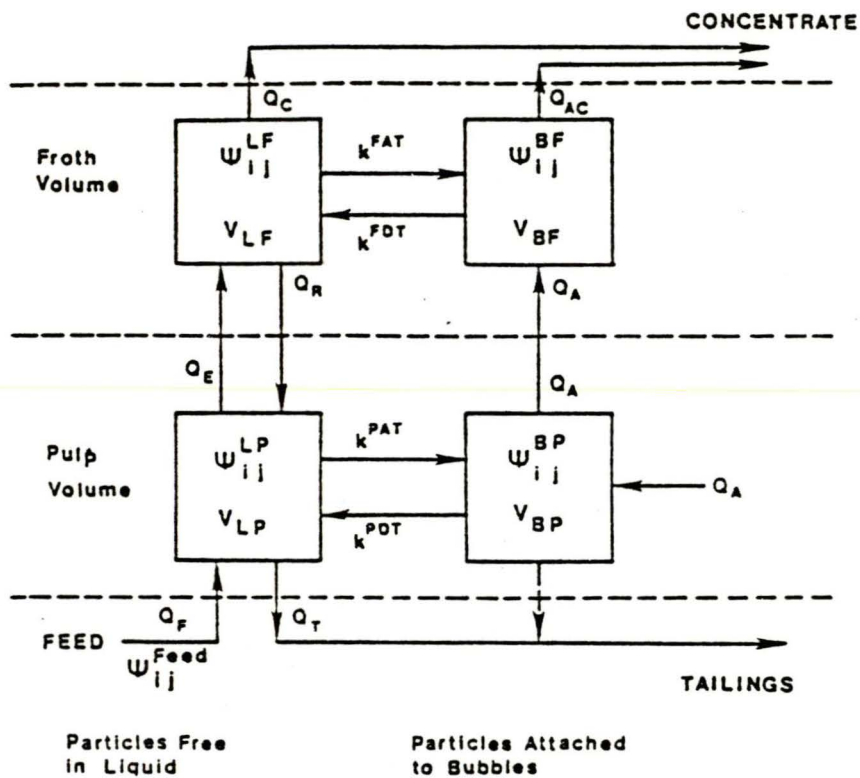


Figure 3. Four states for particles in a flotation cell:

- 1) Free in the pulp,
- 2) Attached in the pulp,
- 3) Free in the froth,
- 4) Attached in the froth and associated interphase transfer rates.

description, in the present study the froth zone is assumed to be a lumped, spatially homogeneous zone to minimize mathematical complexity. Further, although a spectrum of bubble sizes exists in a mechanically agitated tank, for simplicity only a weighted average size is considered.

Particle Flotation Model

Population balance concepts have been shown to be of great utility in describing the behavior of assemblies of particles in complex processes (18,19) including grinding, pelletization, leaching, roasting, crystallization, fermentation, etc. For systems which are reasonably well mixed or for which flow patterns are complex, macroscopic population balance models (PBM) have been found to be most useful. This type of model, applied to particles in each of the four states depicted in figure 3, will be used here to form a framework for describing flotation cell behavior.

The macroscopic PBM equation can be written in its most general form as follows (18):

$$\frac{1}{V(t)} \frac{\partial}{\partial t} [V(t)\psi(t)] + \sum_{i=1}^m \frac{\partial}{\partial \xi_i} [v_i \psi(t)] + D(t) - B(t) = \frac{1}{V(t)} \left[\sum_p Q_{IN}^{(p)} \psi_{IN}^{(p)}(t) - \sum_q Q_{OUT}^{(q)} \psi_{OUT}^{(q)}(t) \right] \dots\dots\dots(1)$$

In equation 1, $\psi(t)$ represents the number density of particles in a specified state with property values in the ranges ξ_i to $\xi_i + d\xi_i$. The first term in this equation represents the accumulation of species in any volume $V(t)$, and the second term takes into account continuous changes of particle properties within the volume, while D and B represent discrete death and birth rates of particles in the volume, and the terms on the righthand side represent the input and output flow rate

of particles across the boundaries of the volume under consideration. The particle properties of the greatest importance in flotation are size and composition. In this regard $\xi(t)$ in Equation 1 is taken to be $\xi_{ij}(t)$ where interval i is a narrow size range and interval j is a narrow range of mineralogical compositions; therefore $\xi_{ij}(t)$ gives the number of particles of "size i " and "mineralogical composition j " per unit volume in any specified state in the flotation cell.

The application of Equation 1 to each of the four states 1) free in the pulp, 2) attached in the pulp, 3) free in the froth, and 4) attached in the froth leads to the set of differential equations given in table 2. In each case flows into and out of a volume (Q) are considered to carry particles as depicted in figure 2, while attachment and detachment processes are represented as birth and death terms characterized by rates which are proportional to the number of particles present in a given phase, with attachment and detachment rate constants k^{AT} and k^{DT} determined by molecular, electrostatic, and hydrodynamic forces. It is recognized that a death event in one phase results in an immediate birth event in the complementary phase in the same volume. Finally, the properties of a given particle in the cell are not considered to be time-dependent, so that term two in Equation 1 is zero in all cases. The set of coupled differential equations given in table 2 should provide a complete description of particle dynamics in a flotation cell. In order to implement these equations, the forms of rate constants for attachment and detachment must be specified and a model for the water flows must be provided.

Table 2. Population Balance Model for Four States in a Flotation Cell

Free in the pulp

$$\frac{d}{dt} (V_{LP}\psi_{ij}^{LP}) + k_{ij}^{PAT} V_{LP}\psi_{ij}^{LP} - k_{ij}^{PDT} V_{BP}\psi_{ij}^{BP} = Q_{Feed}\psi_{ij}^{Feed} - Q_T\psi_{ij}^{LP} + Q_R k_{ij}^R \psi_{ij}^{LF} - Q_E\psi_{ij}^{LP} \dots(2)$$

Attached in the pulp

$$\frac{d}{dt} (V_{BP}\psi_{ij}^{BP}) + k_{ij}^{PDT} \psi_{ij}^{BP} V_{BP} - k_{ij}^{PAT} \psi_{ij}^{LP} V_{LP} = - Q_A\psi_{ij}^{BP} - Q_{AT}\psi_{ij}^{BP} \dots\dots\dots(3)$$

Free in the froth

$$\frac{d}{dt} (V_{LF}\psi_{ij}^{LF}) + k_{ij}^{FAT} V_{LF}\psi_{ij}^{LF} - k_{ij}^{FDT} V_{BF}\psi_{ij}^{BF} = Q_E\psi_{ij}^{LP} - Q_R k_{ij}^R \psi_{ij}^{LF} - Q_C \psi_{ij}^{LF} (4)$$

Attached in the froth

$$\frac{d}{dt} (V_{BF}\psi_{ij}^{BF}) + k_{ij}^{FDT} V_{BF}\psi_{ij}^{BF} - k_{ij}^{FAT} V_{LF}\psi_{ij}^{LF} = Q_A\psi_{ij}^{BF} - Q_{AC} \psi_{ij}^{BF} \dots\dots\dots(5)$$

Rate Constants in Particle Balances

Attachment Phenomena in the Pulp.

Mika and Fuerstenau (10) have critically reviewed the various viewpoints presented in the literature concerning attachment subprocesses. Other reviews have been presented by Laskowski (20) and by Jameson, Nam, and Moo Young (21). The formation of a particle-bubble aggregate proceeds via three important steps: 1) approach of a particle to a bubble; 2) thinning of the water film between particle and bubble; and 3) receding of the residual film to given an air-solid interface.

The most relevant approaches to deriving a net attachment rate constant are those by Woodburn, King, and Colburn (22) and Bishofberger and Schubert (23); both consider the phenomena of turbulence in their development. Bishofberger and Schubert use Abrahamson's (24) equation for aggregate formation, which depends on the local energy dissipation throughout the turbulent velocity regime for the aggregates. The number of collisions per unit of volume and time in a flotation system is given by:

$$Z = 5.0 N_{ij} N_B d_{iB}^2 U_t \dots\dots\dots(6)$$

where N_{ij} and N_B are particle and bubble number, respectively, available for collision, and d_{iB} is the mean size of the aggregate of size i (particle-bubble). The turbulent aggregate velocity, U_t , which they use is that proposed by Liepe (23), i.e.,

$$U_t = k_t \epsilon^{4/9} d_{iB}^{7/9} [(\rho_j - \rho_p) / \rho_p]^{2/3} (\rho_p / \mu)^{1/3} \dots\dots\dots(7)$$

where ϵ is the average energy dissipation in a flotation given by P_g / V_{LP} in our treatment, ρ_j is the specific gravity of species j , ρ_p is the specific gravity of the pulp, and μ is the viscosity. Comparison of Equation 8 with the second term in the Equation 2 yields

$$k_{ij}^{PAT} = k_{ij}^{PAT} V_{BP} d_{iB}^2 U_t / d_{BP}^3 \dots\dots\dots(8)$$

where k_j^{PAT} needs to be determined experimentally for each mineralogical species. The mean bubble diameter is determined with the Calderbank (25) modified equation.

The Woodburn, King, and Colborn equation for this rate constant is

$$k_{ij}^{PAT} = k_j^{PAT} \phi(D) AS \dots\dots\dots(9)$$

where k_j^{PAT} is a constant for mineral species j , $\Phi(D)$ is a function which accounts for the influence of particle size, A is the total bubble-surface area per unit of pulp volume, and S is the fraction of the surface area of a single bubble that is not covered by adhering solid particles. In our treatment the part of the function $\Phi(D)$ that corresponds to dislodgement of adhering particles was not considered in the attachment process but rather was taken into consideration in the detachment step. As a first approximation, S can be taken as unity and A can be estimated for spherical bubbles by $A = 6\phi_p/d_{BP}$ in which case the following expression results:

$$k_{ij}^{PAT} = k_j^{PAT} \frac{\phi_p}{U_R^2} \frac{d_{BP}}{d_p} \exp\left(-\frac{\chi d_{BP}}{U_R d_p^2}\right) \dots\dots\dots(10)$$

where U_R , the relative velocity between bubble and particle, was once again estimated by Liepe's turbulent velocity, χ is a proportionality constant, d_{BP} is the mean bubble diameter estimated with the Calderbank modified equation (25), d_p is the particle size, and ϕ_p is the air hold-up in the pulp volume. Both Equations 8 and 10 have been evaluated in the current study.

Detachment Phenomena in the Pulp.

A well-documented review of different approaches that have been used to quantify the detachment mechanism in flotation is presented by Mika and Fuerstenau (10).

It has been shown that the upper size of flotability in an impeller flotation machine is determined by agitation with turbulence as the characteristic parameter (26). Schulze points out the dominance of tensile forces, both turbulent tensile and shear strengths acting in the

aggregates as a function of the specific energy dissipation. Mika and Fuerstenau (10) derived an expression for the detachment process based on Thomas's argument (27), which has the following form: $d_{ij}^{PDT} \propto \epsilon^{1/3} d_p^{7/3}$, assuming constant aeration in the use of ϵ . Woodburn, King, and Colburn derived an expression based on the maximum deformation stress set up in the bubble skin following a sudden acceleration of the bubble-particle. They obtained the following proportionality for the probability of detachment: $P_d \propto d_p^{1/5} U_0$, where U_0 is the instantaneous velocity achieved by a bubble due to its interaction with an eddy. By analogy, in general in a flotation cell the specific detachment rate as a function of size can be expressed as

$$k_{ij}^{PDT} = k_j^{PDT} d_p^n U_t \dots\dots\dots(11)$$

where U_t is the turbulence velocity given by Liepe's equation and n is an adjustable parameter. In this model, the rate of detachment depends on the surface shear and the size of the particle. The shearing stress depends on the turbulence velocity U_t .

Attachment Phenomena in the Froth.

If inadequate frother is added to a flotation cell, extensive disruption of aggregates occurs in the froth due to bubble bursting with subsequent loss of particle load. These particles may be reattached in the froth or may drain back into the pulp, depending on the operating conditions. The bursting of bubbles not only occurs if inadequate frother is used, but other variables may contribute to the instability of the froth, such as inadequate mechanical removal of the froth or the presence of particles which form a very small contact angle with the air phase.

To derive an expression for the attachment in the froth, a flow-line

interception mechanism of particle collection has been assumed. In this regime, the efficiency of collection is given by the ratio d_p/d_{BF} , where d_p is the diameter of a particle and d_{BF} is the diameter of a bubble in the froth. This collection mechanism has been described by Gaudin (28) and has been supported experimentally by Spedden and Hannan (29) in a highly idealized flotation study which resembles the process occurring in the froth. Under these conditions, the rate of attachment of particles in the froth will be given by the number of bubbles per unit of time that rise throughout the froth of height H_F , multiplied by the efficiency of collection by stream-line interception. The equation for the rate constant of attachment in the froth can be written as:

$$k_{ij}^{FAT} = k_j^{FAT} Q_A \left(\frac{d_p}{d_{BF}}\right) \cdot \left(\frac{H_F}{d_{BF}}\right) \dots\dots\dots(12)$$

in which the first term in parentheses on the righthand side represents the collision efficiency and the second the number of "bubble heights" in the froth.

Detachment Phenomena in the Froth.

The argument used to postulate a detachment rate-constant equation for the froth is based on the fact that the particles which are attached to a bubble experience a shear force exerted by the fluid draining past a surface in the downward direction; the larger the particle, the larger the force for disruption. The other effect considered is that due to gravity. The resulting equation has the following form (30):

$$k_{ij}^{FDT} = k_j^{FDT} \rho_j d_p U_\infty \dots\dots\dots(13)$$

where ρ_j is the specific gravity of mineralogical species j and U_∞ is the bulk-fluid velocity occurring as a result of drainage. This

equation is derived for flow in the Stoke's regime. A similar expression can be developed by considering the torque required to dislodge a single particle from the surface of a bubble (30). In both derivations, the water drainage velocity U_{∞} can be approximated by

$$U_{\infty} = Q_R/A_3(1 - \phi_F) \dots \dots \dots (14)$$

where Q_R is the volumetric drainage rate, ϕ_F the air hold-up in the froth and $A_3(1 - \phi_F)$ represents the effective cross-sectional area of the liquid phase in the froth.

To complete the description of a continuous flotation cell, a predictive expression for the distribution of liquid between the pulp and froth is required. This expression will be obtained by postulating a hydraulic model for the flotation cell.

Hydraulic Model

Early workers concerned with the modeling of the flotation process generally concentrated on the behavior of valuable particles and tended to neglect the behavior of gangue particles and water. Recent investigators have begun to recognize the importance of including water behavior in flotation models (31). Empirical entrainment models for gangue recovery have been used by Lynch (11), and Moys (13) has given a first-approximation model for the distribution of water in the flotation cell. One of the most important factors that controls the water distribution in a flotation cell is the froth. Unfortunately there has been very little consideration of water and particle transport in the froth (13,31,42), even though the froth and associated drainage phenomena are considered to be the principal reasons (32) for the cleaning action of the cell. The approach used here in modeling water

transport through the froth assumes that bubbles leaving the pulp carry a sheath of water which moves into the froth. The size of the bubbles and the thickness of the water sheath is determined by surface tension and agitation conditions in the pulp. Drainage of water back into the pulp is modeled by analogy with drainage through bubble plateau borders in foams. The height of the froth is determined by the froth removal mechanism. The development of the necessary equations is given below.

Consider again figure 2 in which the volumes V_{LP} , V_{BP} , V_{LF} , and V_{BF} are, in general, time-dependent. Most dynamic studies in flotation have considered constant volumes (6,8,9,11), but in order to include changes in froth height and pulp level in the present study, a time-dependence must be incorporated for these quantities. To a first approximation, the liquid volumes are not influenced by the floatable particles (10); therefore this complication was ignored.

In order to quantify the interphase transfer of water Q_E , Q_R , Q_C , and of air Q_{AT} , Q_{AC} , a study of the water and air behavior in the flotation cell was made. A general water volume balance in the flotation cell yields:

$$\frac{d}{dt} (V_{LP}) = Q_{Feed} - Q_T - Q_E + Q_R \dots \dots \dots (15)$$

$$\frac{d}{dt} (V_{LF}) = Q_E - Q_R - Q_C \dots \dots \dots (16)$$

Although equivalent expressions can be written for the air phase, it will be assumed here that the air-phase dynamics need not be modeled since changes in air volumes occur very fast compared to the water volumes and therefore steady-state values can be used.

Water Model

Water Entrainment.

An attempt to derive an expression for the water entrainment rate into the froth, Q_E , has been made by Mika and Fuerstenau (10) based on observations by Klassen and Tikhonov (33). The latter investigators proposed that a major proportion of water and nonfloatable fines which cross into the froth are entrapped in a "boundary layer" of water around the bubble. A similar approximation was made in Moy's froth model. This concept has been used by Derjaguin and Dukhin (34) to explain the attachment of fine hydrophobic particles in flotation. Bubble boundary layers have been studied extensively in a fluidized-bed reactor design because of their effect on reaction kinetics and elutriation of fines (35). In flotation the magnitude of this boundary layer is apparently controlled by hydration effects at the air-water interface and by the turbulence levels in the pulp volume. The volumetric flowrate of entrained water can be calculated from the number of bubbles rising per unit, $6Q_A/\pi d_{BP}^3$, where Q_A is the volumetric air flow rate and d_{BP} is the mean-size bubble diameter in the pulp region. The volume of liquid held by a film surrounding a spherical bubble is $\pi d_{BP}^2 \delta$, so that the volume flow rate of water into the froth is

$$Q_E = 6Q_A \delta / d_{BP} \dots \dots \dots (17)$$

In order to apply Equation 17, the average value of d_{BP} must be known. Extensive experimentation has been reported on the estimation of bubble size in aerated agitation vessels by Calderbank (25). Some experimental results have been obtained in flotation cells, but no correlation has been given (30). In the current study a modified

expression for the Sauter mean diameter of bubbles in a liquid as proposed by Calderbank has been used, i.e.,

$$d_{BP} = K2 \frac{\phi_p^4 \cdot \sigma_L}{\rho_p^2 (P_g/V_{LP})^4 C_F^{344}} \dots\dots\dots(18)$$

Here σ is the surface tension of the liquid and ρ_p represents the density of the pulp.

The term P_g/V_{LP} in Equation 18 is the power input per unit volume where P_g is the power in the presence of air and V_{LP} of the liquid in the pulp.

Equation 18 arises from the application of the Kolmogorov's theory of local isotropy (36) to aerated agitation vessels, so the form of the equation is universal for systems having similar turbulence conditions. Calderbank introduced the air hold-up, ϕ_p . In this work several different correlations for the air hold-up were tried. Similar experiments to those carried out by Calderbank were done (30). These resulted in the following expression:

$$\phi_p = K3 (Q_A/A_1)^{.67} C_F^{.25} \dots\dots\dots(19)$$

Here A_1 is the interfacial area between the pulp and froth. The Calderbank equation involves surface tension of the liquid but the frother concentration term C_F was introduced by the current authors due to its major effect on the bubble size and the minimum effect of C_F on surface tension at the typical frother addition levels in a flotation cell. Extensive experimentation has been carried out in flotation hydrodynamics concerning the correlation between power and aeration rate (37,38). No correlations that include the effect of frother have been reported. The most complete correlation found in the literature is

(39):

$$P_g/P_0 = C_2 \left[\frac{Q_A}{ND_T^3} \right]^m \left[\frac{N^2 D_T^3 \rho_p}{\sigma} \right]^n \dots\dots\dots(20)$$

where the effect on frother would be reflected in changes in the surface tension, σ . P_0 is the power input where no air is added, which can be expressed as (30):

$$P_0 = C_{\rho_p} N^3 D_T^5 \dots\dots\dots(21)$$

Estimation of the film thickness δ around the bubbles should be done by rigorous hydrodynamic and physicochemical analysis in a flotation cell. As a first approximation, δ can be obtained from hydrodynamic boundary layer correlations available in the literature (40,41). Here the simplest correlation will be used as proposed by Levich:

$$\phi \propto (d_{BP} v_{eff}/U_B)^{1/2} \dots\dots\dots(22)$$

where v_{eff} is an effective kinematic viscosity and U_B is the slip velocity of the bubble through the field. Since the estimation of v_{eff} is very difficult in the system under consideration, it was lumped into an overall constant. For estimation of the bubble slip velocity, Levich's approximation for Reynold's numbers above 200 was used, i.e., $U_B \propto (g d_{BP})^{1/2}$ (here g is the gravity acceleration), which is in agreement with the data presented by Clift, Grace, and Weber (41). Unfortunately, no good correlation between U_B and frother concentration is available for the size range of bubbles under consideration (.5 to 1 mm).

Water Drainage.

Mika and Fuerstenau (10) have emphasized that drainage from the froth

is essential to describing the froth concentration process. If redistribution of water within the froth column did not occur, the removal of froth would be impossible because of the drying effect which will upset the froth stability. The inclusion of drainage is fundamental to explaining the observed secondary concentration phenomena in the froth.

Drainage of water from the froth is a complex phenomena which has received very little attention in flotation. Attempts to model this transport subprocess have been made by Barker (42) and more recently by Moys (13). Neither of these approaches has been critically tested. Considerable effort has been put into the description of drainage in particle-free foams (43). Hartland and Barber (44) have derived a model which includes the water that moves upward in the film surrounding the rising bubbles and the water which drains back through the plateau borders (void spaces between bubble contacts) in a column of foam. They have also considered the entrainment of water due to bulk flow of the foam and possible drainage through the films.

The water drainage equation used in the current study was derived following Barber and Hartland (44). Assuming that the water concentrate removal is negligible compared with the drainage from a steady-state analysis, the following return rate can be written:

$$Q_R = Q_A(1-\phi_F)/\phi_F \dots \dots \dots (23)$$

The average liquid to air fraction $(1-\phi_F)/\phi_F$ in the plateau borders, in terms of the total height of the froth H_0 , evaluated at $H_0/2$ is

$$\frac{1-\phi_F}{\phi_F} = \frac{k \delta_c^{6/5} H_0^{14/35}}{(\rho g)^{2/5} \sigma^{2/5} d_{BF}^{12/5}} \dots \dots \dots (24)$$

where δ_c is the critical film thickness (which is difficult to estimate in a system containing particles), d_{BF} the average bubble diameter in the froth, σ the surface tension, ρ the density of the fluid, and g the acceleration due to gravity. The height of the froth was expressed in terms of the volume of liquid in the froth using the relationship $H = V_{LF}/[A_3(1-\phi_F)]$, and Equations 23 and 24 were combined to yield (30):

$$Q_R = KR v^{.53} V_{LF}^{.56} A_3^{.4}/(\sigma^{.24} d_{BF}^{1.92}) \dots \dots \dots (25)$$

where v is the superficial gas velocity (Q_A/A_3), A_3 represent the cross-sectional area of the froth volume, and KR is an adjustable parameter. Finally, an empirical linear correlation between the bubble diameter in the froth d_{BF} and aeration rate Q_A was used.

Water into the Concentrate.

The flowrate of concentrate Q_C must also be modeled to apply to Equation 16. The nature of concentrate removal has been studied by Moys and by Harris and Raja (13,45).

To model this phenomena, the results of studies of flow over a weir were used (46). These basic relationships were modified to incorporate the geometric features of a flotation cell. The correlation developed by Francis, which gives the total volume flowrate of material removed was used to obtain the unforced flow of liquid and solids by multiplying the volume flow by the average liquid content of the froth to obtain the amount of liquid being removed and therefore the mass of particles entrained by the water. The same reasoning was applied for the air volume. The equation used is:

$$Q_C = KC \cdot L \cdot (H_F - H_C)^{1/5} (1 - \phi_F) \dots \dots \dots (26)$$

where L is the width of the flotation cell lip, H_F is the total height of froth referred to the bottom of the cell, H_C is the height of the flotation cell, $(1 - \phi_F)$ is the average liquid holdup in the froth, and KC is an adjustable constant that depends on the type of removal technique used.

*** MODEL PARAMETERIZATION

A pilot-scale flotation circuit has been designed and installed in the Ore Dressing Laboratory at the University of Utah for testing mathematical models and developing control strategies. In the current study the separation of chalcopyrite from gangue was used to test the model described above for both steady-state and dynamic conditions.

Experimental Procedure

Experiental testing for parameterization and verification of a dynamic model for a complicated system such as flotation demands a refined experimental procedure. The size of the test circuit was chosen such that it represents as closely as possible an industrial process, recognizing the constraint that material-handling capability in a university environment is limited. The flotation cell used was a 27 dm^3 (1 cubic foot)¹ cell combined with a 60-dm^3 cylindrical conditioning tank. The major equipment items and instrumentaiton are shown in figure 4. The circuit is instrumented for flow, density, level, on-line particle size, and chemical analysis measurements using standard sensors. A pulp-froth interface detector for froth-height determination and other specialized pieces of instrumentation were developed for this project. All the instruments were calibrated, and feedback control loops for levels, water additions, and feed rate were tuned before

¹Hazen Research, Inc.

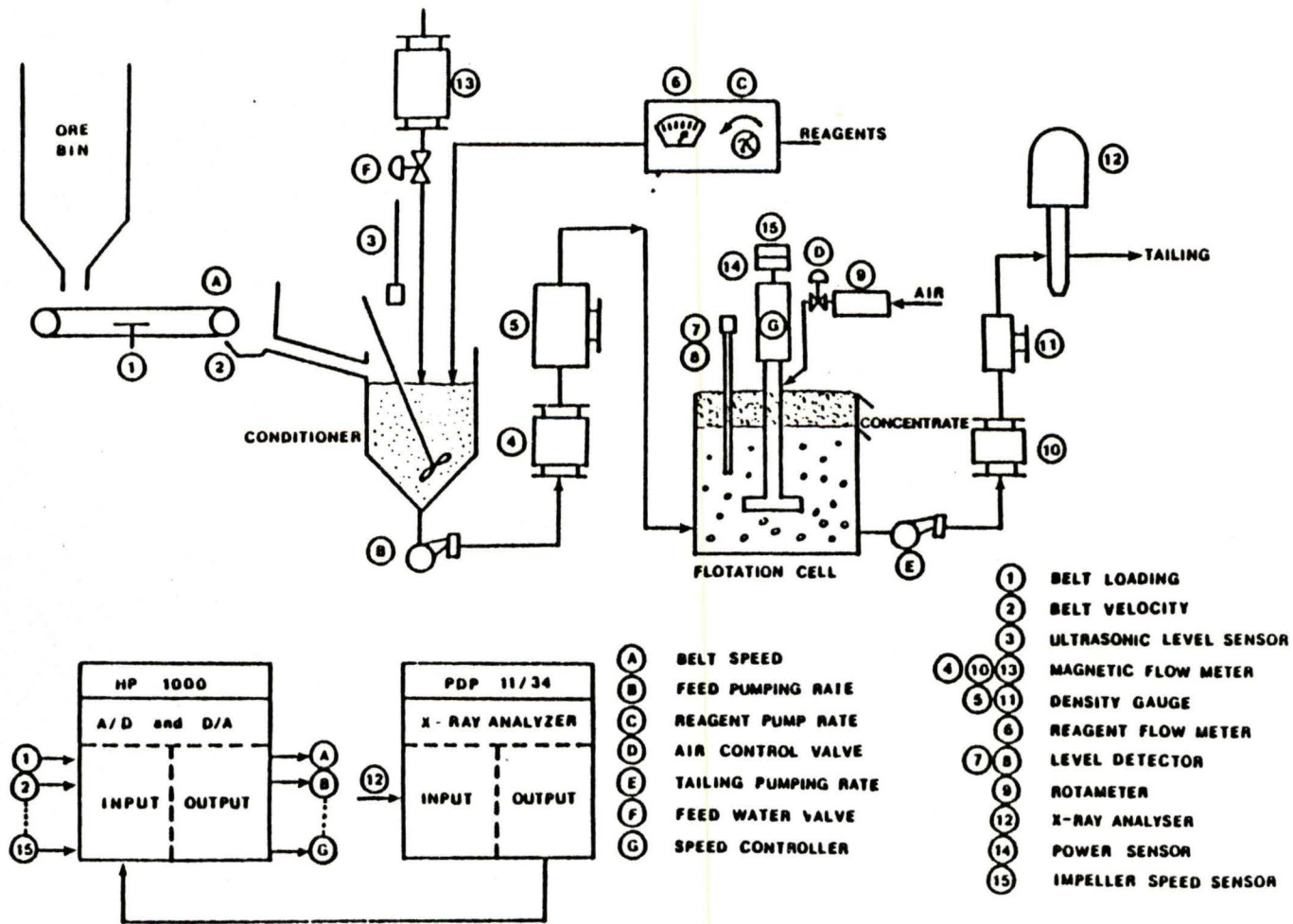


Figure 4. Schematic of pilot flotation circuit including major pieces of process equipment, measurement and control devices.

beginning dynamic data collection.

Two and a half tons of copper sulfide ore were crushed and ground. The product was separated using a 30-mesh U.S.A. screen on a 75-cm (30") SWECO sieving machine. All the undersize material was mixed and stored in plastic bags inside large barrels. One day before each test the required amount of material was loaded into the fine-ore bin.

A series of bench-scale tests and liberation analyses were carried out to define the reagent schedule and size required for the copper sulfide ore, containing 0.975% Cu.

In continuous testing, the system was started up using water only. After steady flows were achieved, the desired solids feedrate setpoint was entered into the computer for the belt-feeder controller. Approximately 15 minutes was required to obtain steady state for the combined solid- and liquid-phase flows. After establishing steady state, a series of step changes in aeration, level of pulp, impeller speed, and mass flowrate of tailings was implemented. Steady-state samples of the resulting tails and concentrate from each run were taken at the beginning and at the end of a run. Steady-state samples from each stream were analyzed for % solids, Cu content, and size distribution. Each size fraction in every sample of concentrate and gangue was analyzed by species, and for copper content. A typical analysis of steady state for one of the experiments is shown in table 3.

The data obtained for each steady state were treated by a program called METABAL to adjust the metallurgical mass balances. This program used a hierarchical mass balance procedure to close the global, per-size and per-species, mass balance. The program allows the weighting of each particular analysis X_j according to its relative reliability and

TABLE 3 TYPICAL STEADY STATE ADJUSTED DATA

COPPER SULFIDE No. B3

1. Experimental Conditions

Aeration rate	35.0	l/min	Impeller speed	950	rpm
Frother concentration	1.02 x 10 ⁻⁴	M	pH	8.7	
Collector addition	10	ml/min	Temperature	18	°C
Depressant addition	0	ml/min	Froth level	40	cm
			Interface level	35	cm

2. Macroscopic Variables

		FEED		CONCENTRATE		TAILING	
		Exp.	Adj.	Exp.	Adj.	Exp.	Adj.
Pulp mass flowrate	g/min	12695	12695		524.56		12170.44
Solids mass flowrate	g/min	2500	2375.97		68.04		2305.96
Percent Copper	%	.975	1.04	19.51	19.51	.5826	.526
Percent iron	%	7.98	8.069	22.15	22.15	5.706	6.68

3. Microscopic Variables

	Size Interval Microns	Size Weight Percent		Copper Percent		Iron Percent		Chalcopyrite		Mixed		Species Weight Percent Gangue		Pyrite	
		Exp.	Adj.	Exp.	Adj.	Exp.	Adj.	Exp.	Adj.	Exp.	Adj.	Exp.	Adj.	Exp.	Adj.
FEED	300/150	31.74	26.87	.8564	.8395	12.27	8.99	1.79	1.88	1.69	1.47	71.77	75.45	24.75	21.20
	150/74	19.88	19.34	.9756	1.2006	7.25	7.45	2.35	2.75	1.17	1.17	82.75	82.75	13.73	13.73
	74/37	20.39	19.92	1.171	1.26	5.99	6.04	3.08	3.26	0.36	0.75	85.53	85.31	10.63	10.68
	-37	27.99	33.87	.9650	1.0659	5.07	4.95	2.75	2.94	0.10	0.14	88.09	87.94	9.05	8.98
CONCENTRATE	300/150	17.52	17.57	17.31	17.31	20.57	20.58	48.00	47.99	5.00	5.00	35.50	35.45	11.50	11.56
	150/174	23.52	23.53	24.04	24.04	26.96	26.96	67.74	67.73	4.25	4.25	15.49	15.50	12.52	12.52
	74/37	21.33	21.33	26.08	26.08	27.34	27.34	74.62	74.61	1.78	1.78	14.10	14.11	9.50	9.50
	-37	37.63	37.57	13.97	13.97	16.93	16.93	40.33	40.32	0.05	0.05	49.62	49.63	10.00	10.00
TAILINGS	300/150	25.98	27.15	.514	.5248	6.73	8.77	1.18	1.00	0.96	1.45	83.52	76.21	14.31	21.34
	150/74	19.09	19.22	.511	.3755	6.88	6.75	1.12	0.385	1.07	1.06	84.06	84.79	13.75	13.77
	74/37	19.76	19.87	.527	.4736	5.39	5.36	1.35	1.00	0.75	0.73	87.14	87.57	10.76	10.70
	-37	35.17	33.76	.703	.6420	4.49	4.56	2.13	1.72	0.20	0.14	89.02	89.24	8.65	8.90

provides the best adjusted values of \hat{X}_i based on a least-squares objective function:

$$\text{minimize } \phi = \sum_i W_i (X_i - \hat{X}_i)^2 \dots\dots\dots(27)$$

$$\text{wrt } \hat{X}_{i1}, Z_i$$

with respect to the adjusted values \hat{X}_i of the measured variable X_i and values of unmeasured flowrates Z_i , under the system mass balance constraints $A(X_i, Z_i) = 0$. Some adjusted values obtained from METABAL can be compared with the actual measurements in table 3.

The adjusted data was then input to a nonlinear estimator and steady-state simulator called ESTIFLOAT to obtain all (twelve) flotation kinetic parameters. A program called WATER was used to obtain the necessary constants (three) for the hydraulic model.

A comparison of the experimental and simulated concentrations of chalcopyrite for the concentrate and tailings of a typical steady-state condition are shown in figure 5. This figure demonstrates that the model accurately represents the size dependence of each species in the flotation cell at steady state.

*** DYNAMIC SIMULATOR

Simulator Development

A flowchart of the dynamic simulator, DYNAFLOAT, is shown in figure 6. The simulator consists of four main modules, each of which is subdivided into appropriate subroutines. The data input module handles all the information required to run the program. The circuit calculation module consists of three major subroutines, the flotation model, the controller, and the integrator, as well as an extra subroutine to calculate the output variables. The subroutine for the

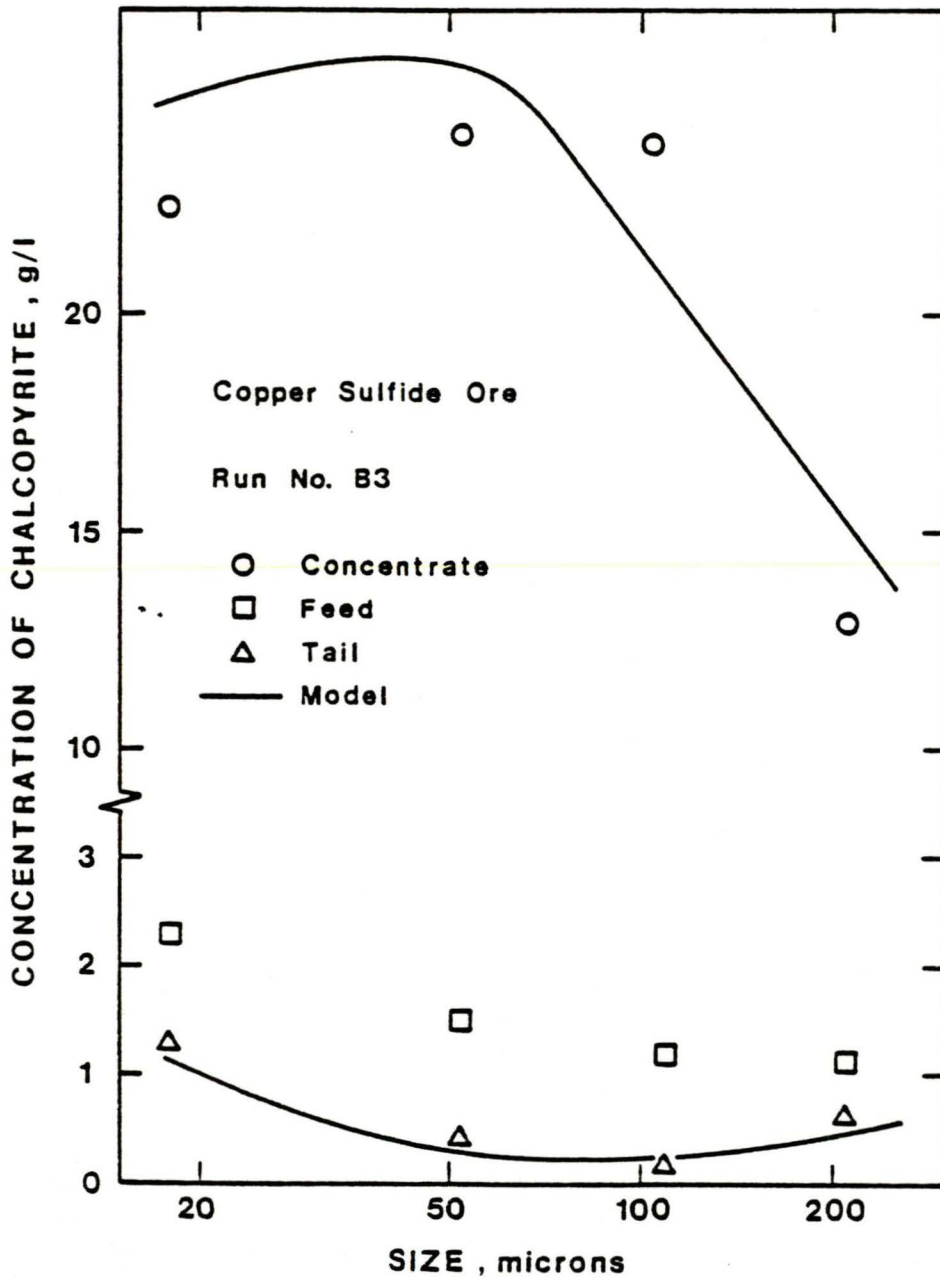


Figure 5. Experimental and simulated concentrations of chalcopyrite in concentrate and tailings by size.

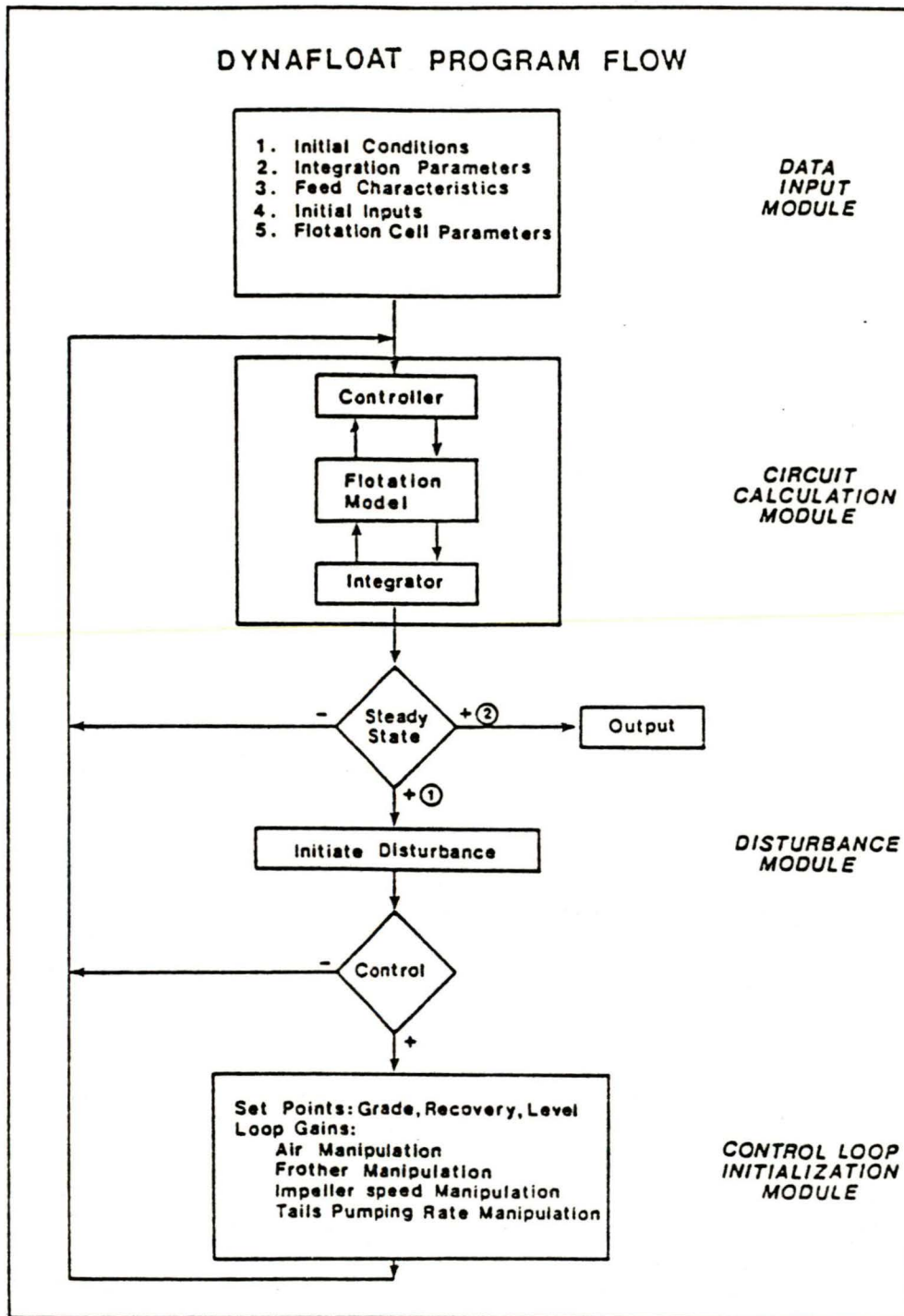


Figure 6. DYNAFLOAT program flowchart.

flotation model combines the particle flotation model with the model for cell hydraulics. Each size and mineralogical species is described by a set of four differential equations plus the water model. The controller subroutine consists of a general proportional-integral controller which allows the coupling of manipulated variables including aeration rate, impeller speed, frother addition, pumping rate of tailings, together with controlled variables, including recovery of valuable species, grade, mass flow rate in the concentrate of valuable species, and pulp level in the flotation cell. There are also options to cascade the grade of valuable species with the pulp level to obtain the froth height by manipulation of any of the variables described earlier. The integrator subroutine uses a 4th-order Runge-Kutta method for solving the overall system of nonlinear differential equations. The disturbance module allows for introduction of random and/or deterministic disturbances to analyze dynamic responses or for testing of control strategies. The control-loop initialization module is called when different possible control strategies are to be analyzed.

The program has been written in BASIC and in FORTRAN. The BASIC program is written for use in an interactive mode. The computer program asks for options to be exercised, i.e., dynamic simulation, control, and parameter inputs. A CRT display shows the evolution of the process in a schematic representation of a flotation cell. The pulp and froth volumes have different colors and pulp level and froth depth changes depending upon the operating conditions. The program written in FORTRAN, which uses an edit file for input, is faster and can handle more sizes and species and allows for making random disturbances in time.

There are certain peculiarities in the model which make computations

difficult especially when the species under consideration is a slow floating nonvaluable mineral. In this case, the rate of attachment is very slow compared to the rate of detachment producing a condition referred to as stiffness in the differential equations. These equations required special treatment. In this study the mechanism of attachment and detachment for the gangue was neglected, and its behavior was represented entirely by the entrainment and drainage mechanisms. Additional work is being done to deal with the stiffness of the equations numerically.

Simulator Verification

The simulator was tested against experimental responses by subjecting it to the same feed conditions and disturbances experienced in experimental runs. The feed disturbances and manipulated-variable values which were stored on the HP 1000 were input at one-minute intervals through the disturbance module of the simulator, and the dynamic response was calculated. Parameter values were those obtained from the steady-state data shown in figure 4.

Figure 7 shows the dynamic response of the flotation cell to stepchanges in aeration, tailing removal rate, and frother addition rate. In all instances the simulator predicts quite accurately the transient response of the mass flow of the tailings (MT) and concentrate (MC), the percent solids in the tails (ST), and the grade of copper in the concentrate (GRADE). These results suggest that the simulator should be capable of reproducing the essential dynamic characteristics of flotation cell performance for control system development.

Simplified model and verification

Depending upon the application, there are several levels of

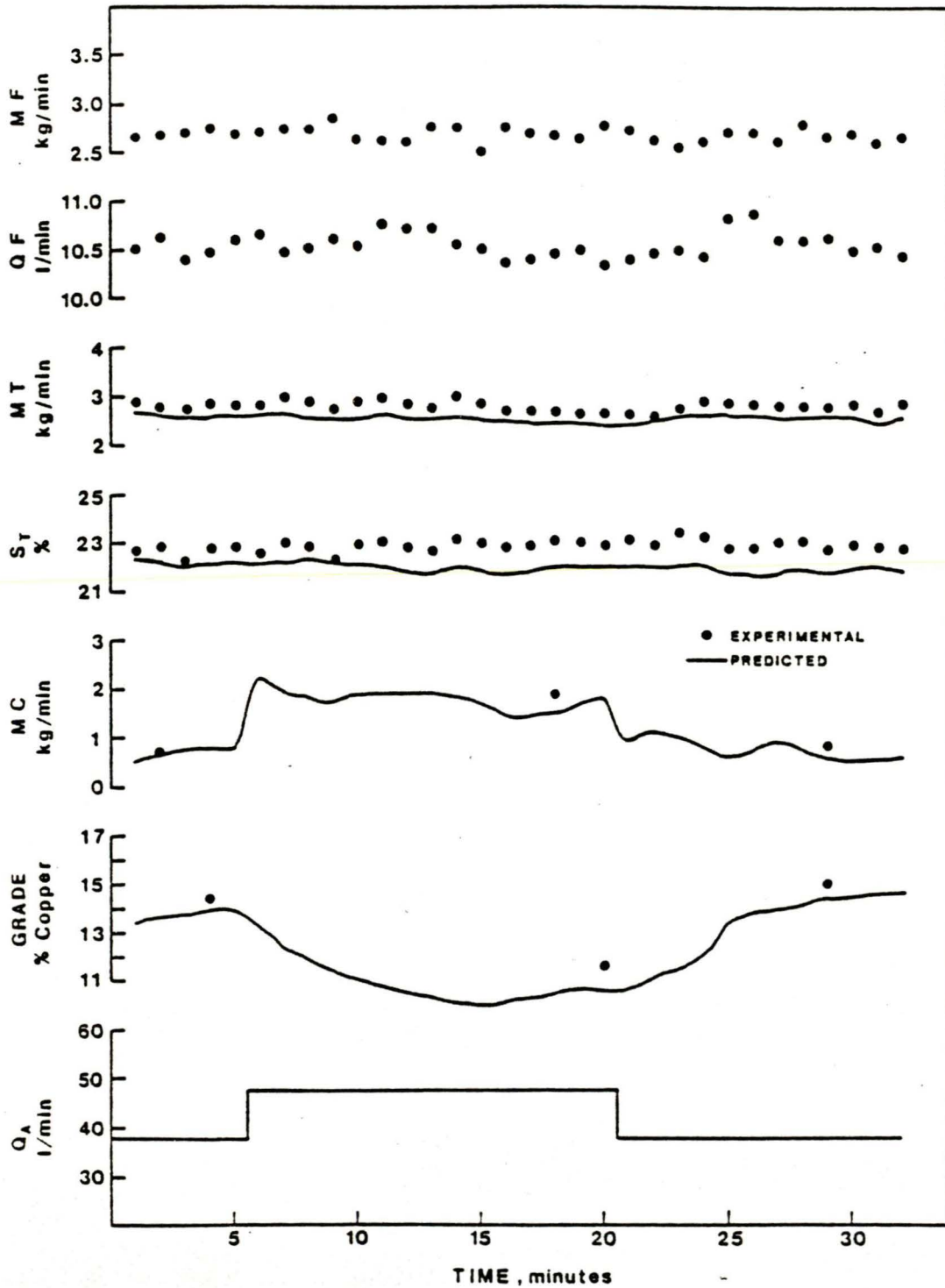


Figure 7. Dynamic verification of the model for aeration changes and feed disturbances for copper sulfide system.

simplifying assumptions which may be of use to develop a simple model for flotation (2).

A first level of simplification reduces the general model by considering that there is a certain physical equilibrium between the particles that are attached to the bubbles and those that are in the liquid both in the pulp and froth volumes. This level of simplification still describes the behavior of the different mineralogical species and particles of different size. The hydraulic description (water equations) remains the same as for the full model. A second level of simplification is obtained by integrating out the effects of particle size, thus averaging particle size effects but maintaining the behavior of the distribution of mineralogical species under consideration.

The set of equations for a mineralogical species j can be written as:

$$\frac{dV_{LP}C_j^P}{dt} = Q_{Feed}C_j^{Feed} - \frac{(Q_E+Q_A\alpha_j^P V_{LP}/V_{BP})}{(1 + \alpha_j^P)} C_j^P + \frac{Q_R k_j^R C_j^F}{(1+\alpha_j^F)} - \frac{Q_T C_j^P}{(1+\alpha_j^P)} \quad (28)$$

FEED	WATER + AIR TRANSPORT	DRAINAGE TRANSPORT	TAILS
------	--------------------------	-----------------------	-------

$$\frac{dV_{LF}C_j^F}{dt} = \frac{(Q_E+Q_A\alpha_j^P V_{LP}/V_{BP})}{(1 + \alpha_j^P)} C_j^P - \frac{Q_R k_j^R C_j^F}{(1+\alpha_j^F)} - Q_C C_j^F \dots \dots \dots (29)$$

WATER + AIR TRANSPORT	DRAINAGE TRANSPORT	CONCENTRATE REMOVAL
--------------------------	-----------------------	------------------------

Equations 28 and 29 represent the balance of mineralogical species j in the pulp and froth volumes, V_{LP} and V_{LF} , respectively. C_j represents the concentration of mineralogical species j while the superscripts P and F are in the pulp and in the froth. α_j^P , α_j^F , and k_j^R are rate

constants in the pulp, froth, and for drainage.

Several sets of simplifying assumptions and methods to obtain the parameters α_j^P and α_j^F are discussed by Bascur (2).

In the simulations that follow, it was not necessary to include any special functional forms for α_j^P and α_j^F for dependencies on species and operating variables. They were obtained directly from the adjusted experimental data using a nonlinear optimization technique (48).

For verification of the simplified model, both steady-state and dynamic data were collected. Steady-state samples from each stream were analyzed for percent solids, percent copper, percent iron and size distribution. Each size fraction in every sample was analyzed by mineralogical species. Microscopic counting of polished sections of concentrate, feed, and tailings samples were used. The following definitions of species were considered in the counting: free chalcopyrite (particles with 95% or more chalcopyrite); mixed material (chalcopyrite and gangue averaging 40% chalcopyrite and 60% gangue); gangue (95% or more silicious material); and pyrite (95% or more pyrite). The minus 400-mesh size fraction was too fine for effective microscopic counting with the instrument available. In this case the chemical analysis was used, and it was assumed that the amount of locked particles in this fine fraction was minimum.

The parameters α_j^P , α_j^F , and k_j^R obtained for the copper sulfide ore using steady-state experiments (Data Set 1) are given in table 4.

TABLE 4. - Comparison of simplified model with experimental data for steady-state copper sulfide ore, experiment B3

Parameter (-)	Chalcopyrite		Gangue		Mixed		Pyrite	
	Exp.	Cal.	Exp.	Cal.	Exp.	Cal.	Exp.	Cal.
α_j^P	1.46		3.78E-5		2.46E-3		1.578E-3	
α_j^F	0.013		4.42E-3		0.0453		0.0253	
k_j^R	0.65		4.0		0.70		3.0	
Concentration (g/l)								
C_j^P	1.87	4.27	198.26	198.11	1.97	2.00	33.02	33.78
C_j^F	83.53	70.91	47.72	52.05	3.42	3.03	16.22	12.32
Solids								
Mass Flowrate (g/min)			Experimental				Predicted	
Feed			2374.00				2284.57	
Concentrate			68.04				76.87	
Tailings			2305.96				2207.70	
Percent Solids (-)								
Concentrate			12.97				12.15	
Tailings			18.95				19.23	
Grade % Copper (-)								
Concentrate			19.51				19.20	
Tailings			0.52				0.62	

An examination of table 2 reveals that the parameters α_j^P and α_j^F for the gangue can be taken to be equal to zero. This table shows that there is very good agreement between the simplified model and the experimental data. Figure 8 shows the dynamic response of the flotation cell to step changes in pulp level and aeration rate for the copper sulfide ore. The prediction of the transient responses are in close agreement with the experimental data.

These parameters were used in the flotation model to derive a Kalman filter for prediction of the unmeasured assays and flowrate in the

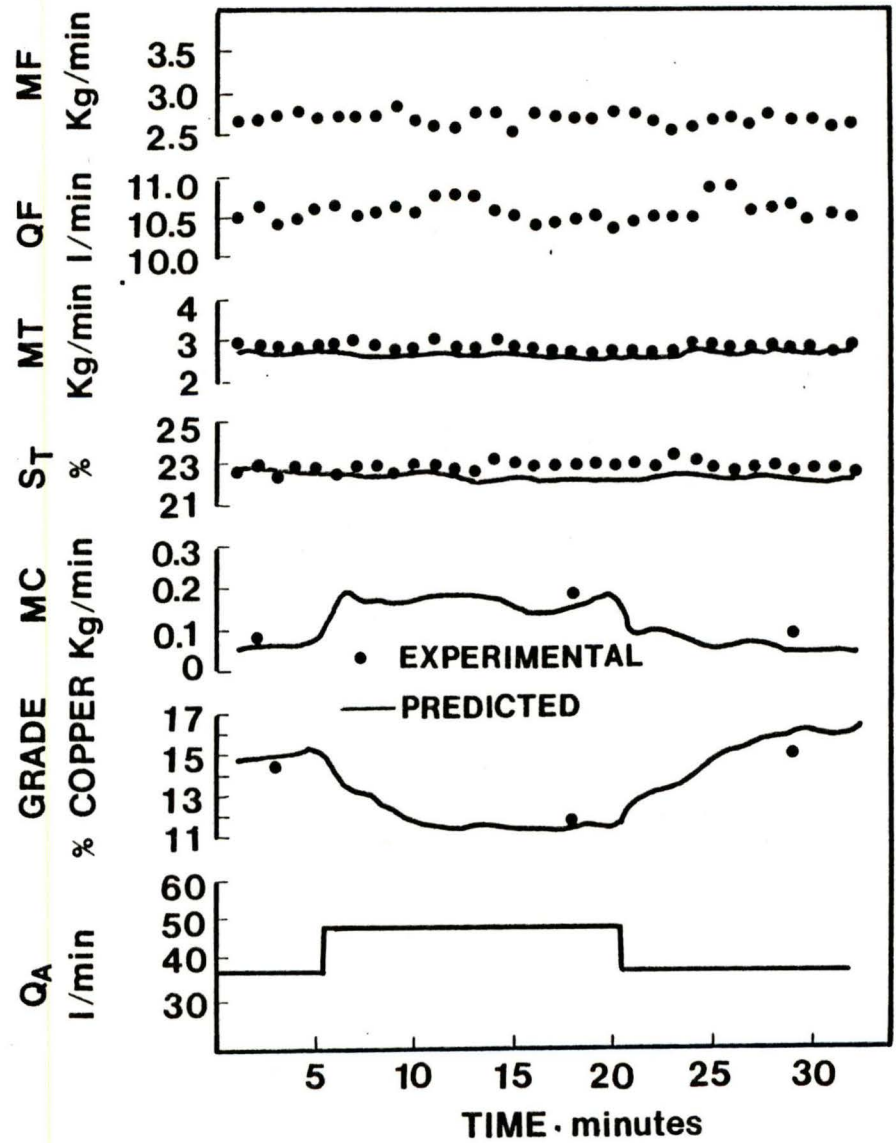
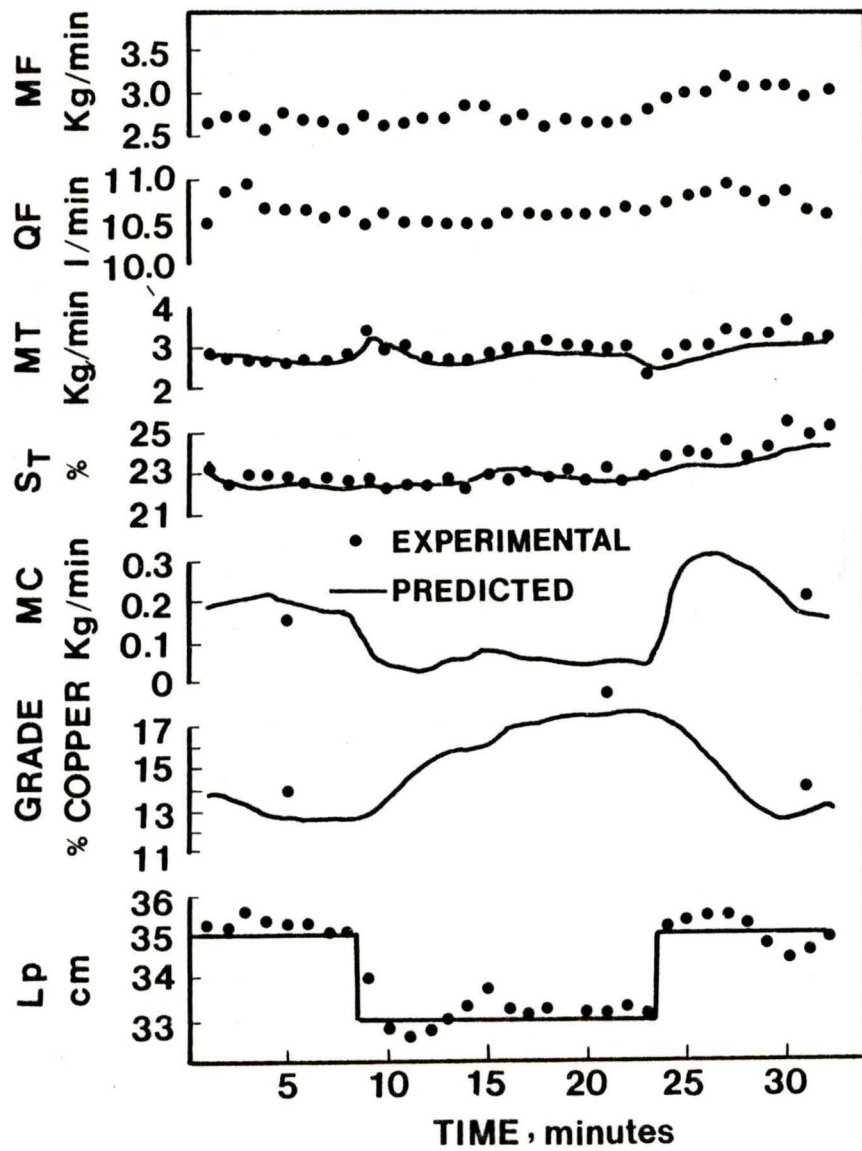


Figure 8. Simplified model dynamic verification.

concentrate from the available information in the tailings stream and the measured variables.

*** DESCRIPTION OF CONTROL STRATEGIES

Implementation of a Kalman filter

The key measurement of the flotation process is made by use of an on-line chemical analyzer (Minexan 202) located in the tailings stream. This measurement results in delays in obtaining chemical assays. In the present system it is impossible to measure the concentrate flowrate and composition which are necessary in order to test control strategies. In order to solve the problem of the undesired time lags within the control loops and to estimate the concentrate mass flowrate and its composition from other measurements, the simplified model along with a Kalman filtering technique for estimation was used.

The Kalman filtering technique uses the available measurements together with the model to filter the noisy data and to predict the unmeasured variables which can be obtained from the model. In addition, this procedure may well be of interest for industrial purposes in the case when it is impossible to install a sampling device in a given stream or when economic restrictions do not allow for the installation of such a unit.

Estimation in conjunction with phenomenological models involves determination of best estimates of the state of the system as well as model parameters. Because the best control can be achieved only when the true state of a system is known at any time, it is important to have the best possible estimate of \underline{x} , the state vector, for use in modern control strategies. The process variables included in \underline{x} can be recursively estimated with an optimal estimator such as the Kalman

filter (49,50) in which the estimates \hat{x} are obtained from the measurement vector, y , and the model predictions according to the following:

$$\hat{x}(k+1) = A \hat{x}(k) + Eu(k) + G(k+1)[y(k+1) - CA\hat{x}(k) - CEu(k)] \quad (30)$$

The lefthand side of the equation represents the new estimate at time $k+1$; the first term on the righthand side represents the predicted estimate based on the previous estimate, the second term represents the effect of input variables, and the last is a correction given by the difference between the new measurements and the predicted measurement based on the old estimate. The measurements and model prediction in the last term are given appropriate weights by the correction matrix G . The correction matrix represents the best compromise between the measurements and model information to obtain the optimal estimate of the state of the system at a given instant. The proper weighting depends on the values of the covariance matrices of the process model Q and the observations R .

In the present investigation, an extended Kalman Filter (51) was used due to the nonlinearity of the process model and measurement models. To analyze the performance of the model and filter, several sampling times of the copper of tailings and percent solids were investigated computationally. The results show that with measurements taken at intervals of up to two minutes, the Kalman Filter is able to track the copper tailing assay quite well and provides reasonable prediction of the (unmeasured) concentrate assay. For sampling time exceeding 3.5 minutes, the performance of the filter decreases considerably. These results were used to set the proper maximum counting time for the XRF

probe for on-line estimation of concentrate copper assay and calculation of the recovery. Figure 9 shows the estimated copper assay and copper recovery in the concentrate obtained with the on-line model-filter from the observation of the percent copper and the percent solids in the tails measurements provided by the XRF probe and the flowrate, level of the pulp taken from the proper instruments.

This analysis suggests that there is considerable potential for this particular model to be applied in industrial flotation plants. First of all, it has an adaptive nature since it is capable of compensating for unknown disturbances reflected in the flotability constants. Secondly, it provides adjusted chemical analysis and unmeasured variables in streams which are difficult to sample. The optimal nature of the state estimates allows for correct accounting of recovery of valuable contents for plant control in transients and steady-state conditions.

Control strategies

On-stream sensing using current instrumentation is limited to the determination of such bulk properties as pulp density, pulp flow, and concentration of selected elements by XRF. In effect any flotation system operating under steady-state conditions involves the composite behavior of fixed proportions of a given number of separate components, each with definite characteristics as described earlier. Neglecting changes in equipment performance, changes in the flotation circuit performance must be caused by a change in the number of components, behavior characteristics, or combinations of these, and it is essential to determine which is the source before the right corrective or control action can be taken. It is doubtful whether this can be achieved by the measurement of bulk properties except for relatively simple systems.

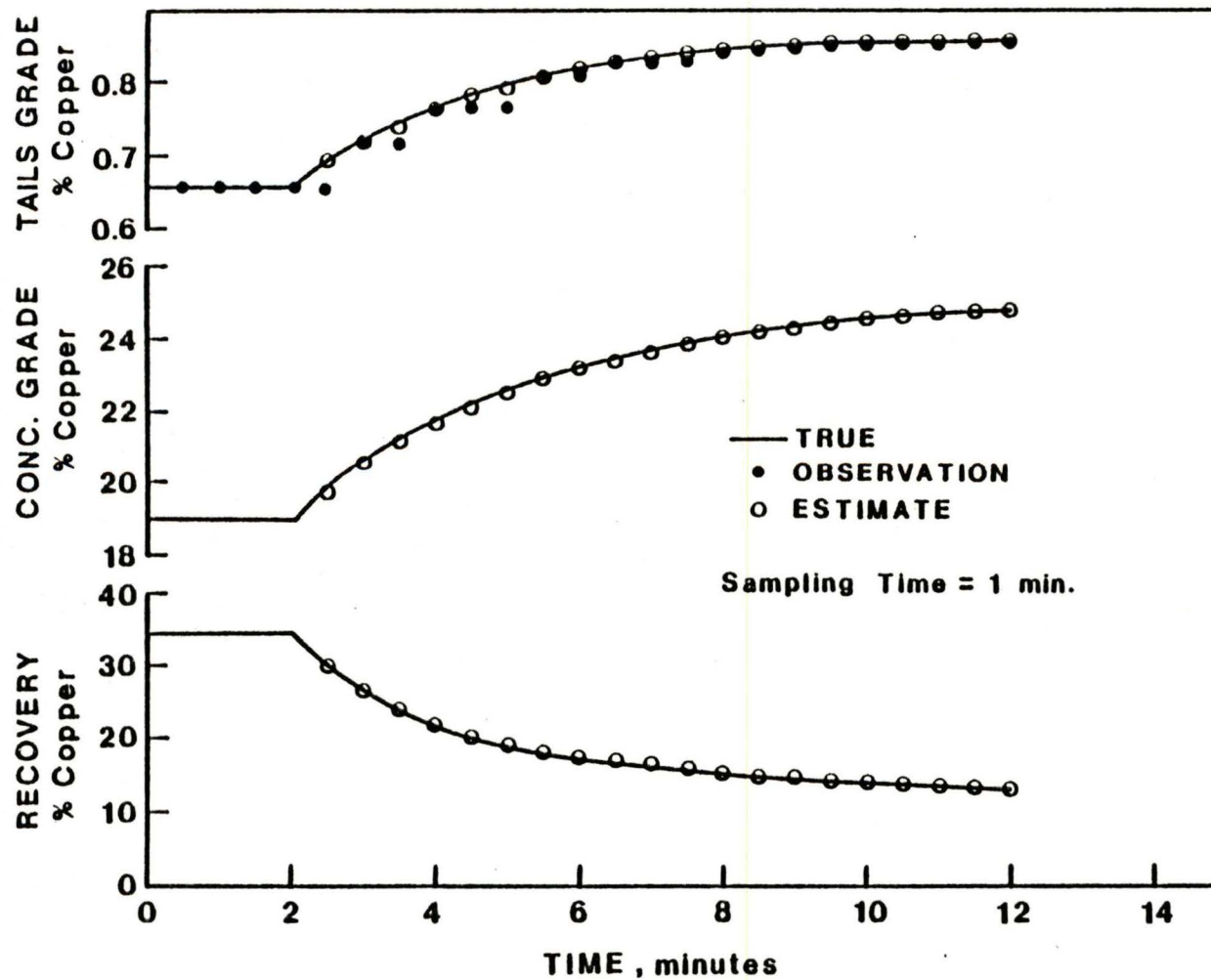


Figure 9. Estimation of concentrate grade and recovery of copper from measurement of tailing % copper using Kalman filter.

The phenomenological flotation model developed by the authors can be used to solve some of these current problems, and the on-line simplified model provides the basis for several model-based control strategies.

In practice, the alteration of flotation rates is accomplished by changes in reagent additions, rate of aeration, and/or pulp level. Determination of the amount of control action to be taken necessitates a knowledge of quantitative relationships which must be established by proper modeling and experimentation in a particular circuit. While it is possible to determine, for example, the empirical relationships between flotation rate constants and reagent additions, aeration rates, pH, and other variables and hence select optimum conditions for one run of ore, it does not follow that the same relationships can be used to determine the level of corrective action to be taken to compensate for a change in ore properties. This is the way the adaptive nature of the proposed model-based formulation is so valuable in flotation systems.

The initial step in the analysis of alternative strategies of control is the classification of important variables for copper sulfide ore flotation (see table 1).

Manipulated variables for any flotation process can be classified into two categories, chemical and physical. The chemical-variable category includes reagent addition rates, addition point of reagents, and collector-modifier ratios. In the physical category of manipulated variables, aeration rates, agitation, pulp level, and conditioning time are the most important ones.

By using a dynamic simulator, a qualitative indication of how manipulated variables influence three main controlled variables of a copper sulfide system was obtained. In this regard, DYNAFLOAT the

computer program based on the full flotation model) (2) was subjected to a series of step changes in manipulated variables, and the direction and the speed of the response of controlled variables were observed computationally. The results of these computations are shown in Table 5. In this representation, termed the process matrix (52), the response of a controlled variable (column) to a change in a manipulated variable (row) is indicated at the row and column intersection. A "+, 0, or -" refers to the direction of change in a control variable. In addition, since the speed of response to control actions is important, this is indicated for each entry by "F" or "S" (fast or slow). It is important to emphasize that, in most instances, a change in one manipulated variable will result in a simultaneous change in all the controlled variables. Such interactions are undesirable, but unavoidable in single-input/single-output control strategies. The process matrix, even in this qualitative form, contains considerable useful information for the design of a control system for the particular ore treated in this study.

TABLE 5. - Response of controlled variables to changes in some manipulated variables as indicated by the process matrix

<u>Manipulated Variables</u>	<u>Controlled Variables</u>		
	Grade	Recovery	Froth Depth
Aeration rate	S ⁻¹	F ⁺²	F+
Pulp level	S-	S+	S+
Impeller speed	S0-	F+-	S-
Frother addition rate	S-	F+	F+
Collector addition rate	S-	S+	S-

¹S = slow

²F = fast

Grade of chalcopyrite controller. From the process matrix developed for copper sulfide flotation, the grade needs a special type of control because of its slow response to the five manipulated variables analyzed. The objective of this controller will be to increase the speed of response. Two alternatives were analyzed; the first one considers the grade-level combination in which the level setpoint is cascaded from the grade controller to finally set the tailings removal rate. The second alternative considers a grade-air controller with constant level and impeller speed compensation to maintain constant power (53). Both strategies are presented in figure 10. An analysis of the two strategies shows that the copper-grade response speed can be increased by manipulating either variable, level having a shorter settling time.

Recovery of Chalcopyrite Controller.

For this controller two manipulated variables were investigated, aeration rate and pulp level. The responses of both controllers are shown in figure 11. The aeration rate controller was tuned with constant level and impeller speed compensation, so the power stays constant when the air is manipulated. Notice that both responses are quite fast, the recovery-level settling needed 2.5 minutes, while the recovery-air needs seven minutes due the interactions with the level controller. In both strategies the grade has a very slow response. The setpoint change introduced from 38.6% to 43% chalcopyrite recovery is quite large for this system. This is apparently the reason why the grade reacts so slowly.

The control strategies presented above represent alternative control strategies evaluated using the flotation dynamic simulator DYNAFLOAT for

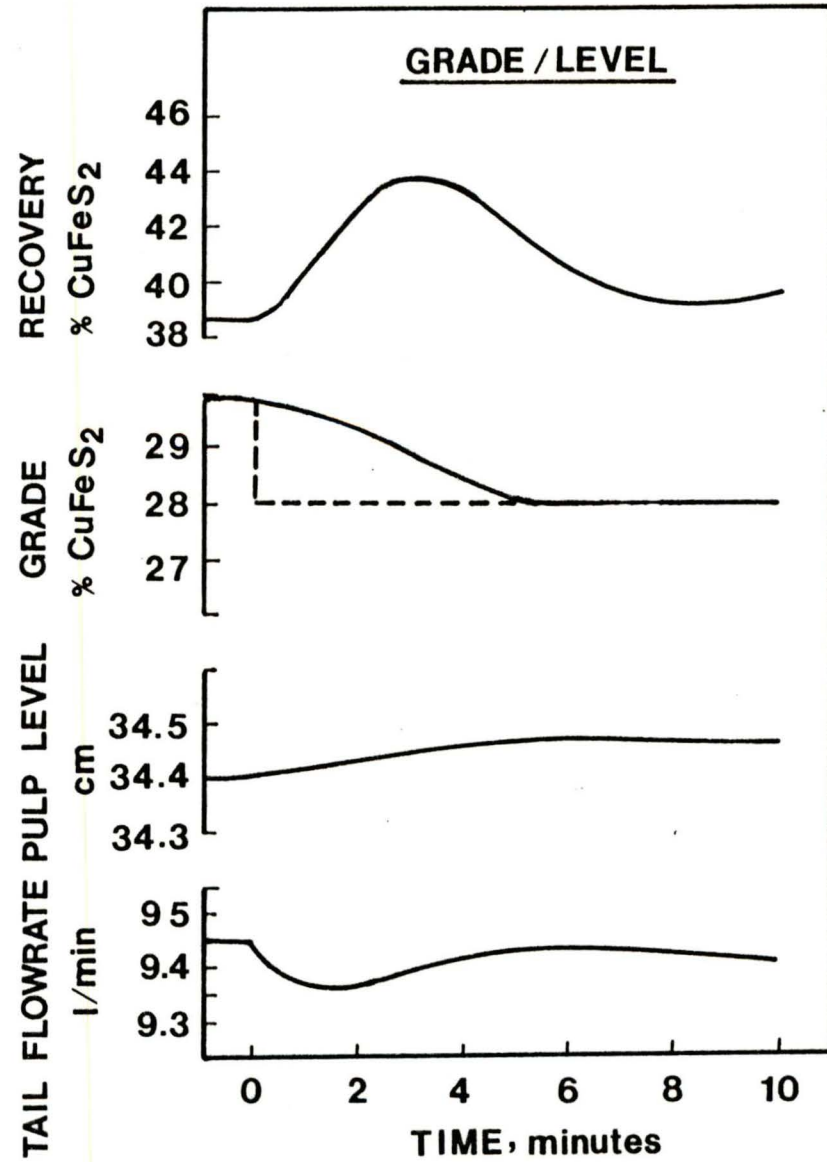
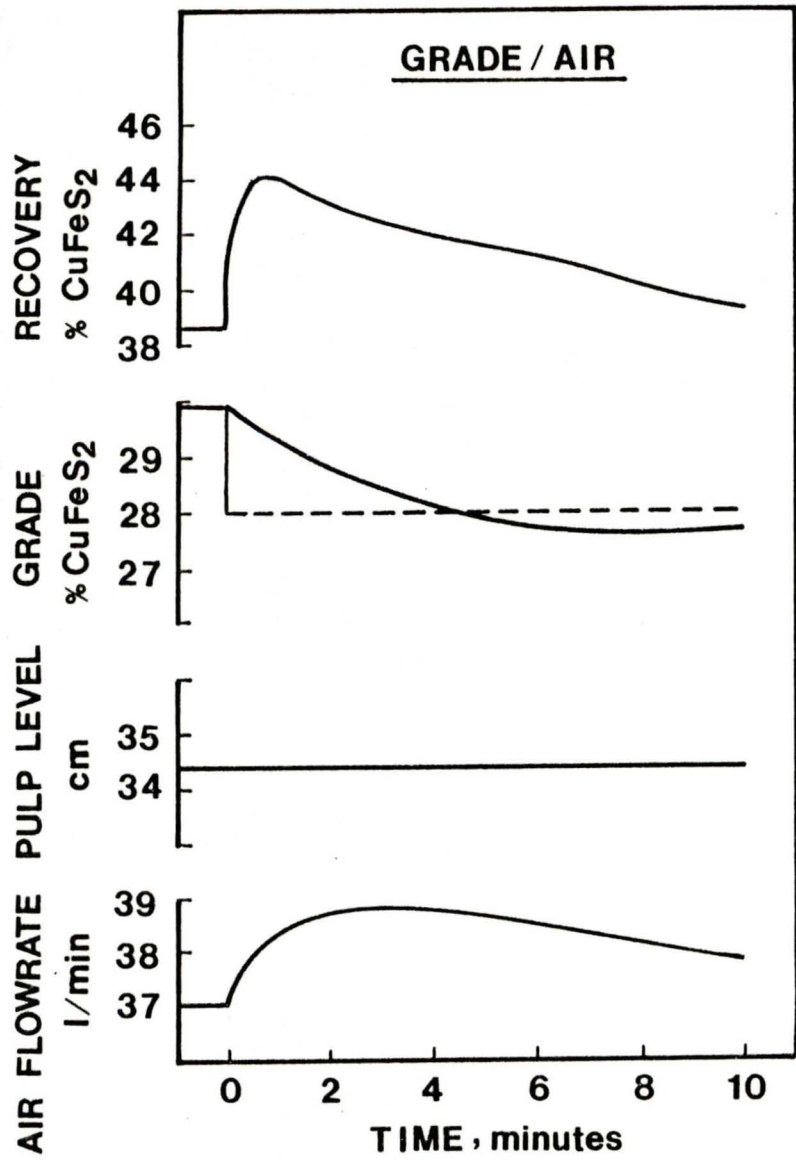


Figure 10. Simulated grade-air and grade-level control loop responses of recovery and grade.

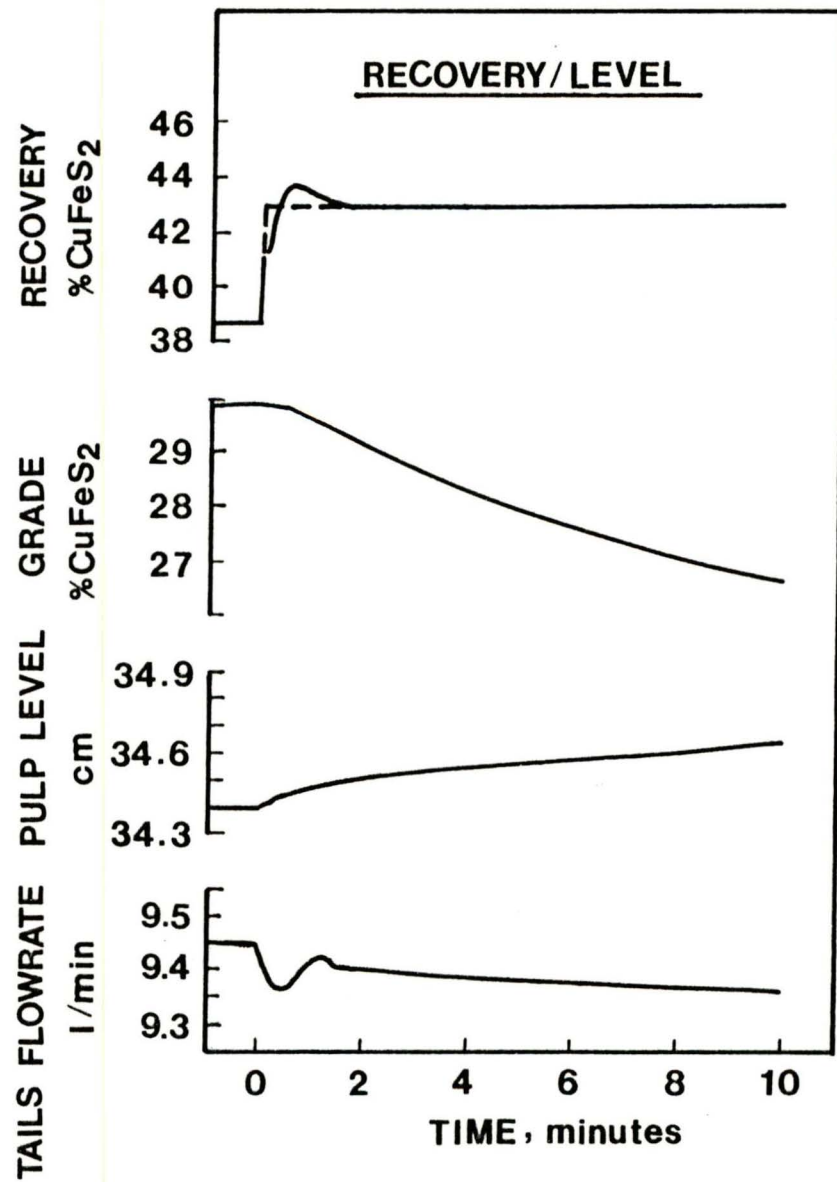
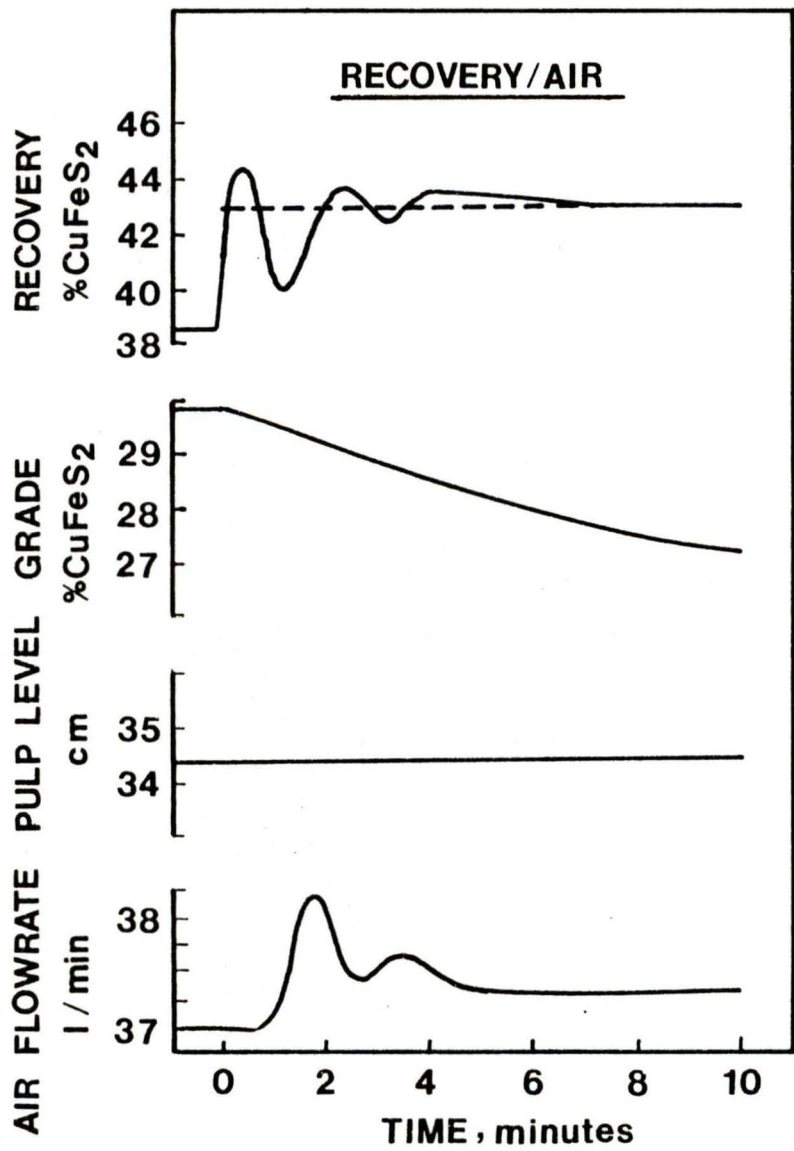


Figure 11. Simulated recovery-air and recovery-level control loop responses of recovery and grade.

a single cell. An extension to the behavior of a rougher-flotation-circuit performance can be easily achieved. From this analysis it is concluded that grade-level and recovery-air represent a good coupling of variables when the circulating loads are small or inexistent.

On-line Sensing of Ore Characteristics

McKee, Fewings, and Lynch (54) have identified that, for the implementation of a flotation control system, it is important to sense as soon as possible that a change in ore type, that is, a change in mineral "floatabilities," has occurred in order to be able to take corrective action quickly. These investigators propose to fully instrument the first few cells in a rougher bank which responds quickly to a change in ore type. A refinement of their suggestion can be made by implementing an on-line flotation model in only one fully-instrumented cell to evaluate quantitatively the flotation rates and other unmeasured variables in the flotation process. Using the available on-line flotation model-filter, a powerful technique can be implemented for effective corrective actions to be taken as soon as possible in the flotation system. With the availability of a predictive dynamic model for flotation, a new flotation circuit control strategy results (see figure 12). For implementation of the model-based control strategy, the rougher bank can be divided into two sections. The behavior of the first few cells in the rougher bank responds quickly to a change in ore-type; by feeding this information to the on-line model, the unmeasured variables and parameters can be obtained. Thus, the floatability of the ore can be estimated early in the circuit to take corrective actions in the cleaners and scavenger units.

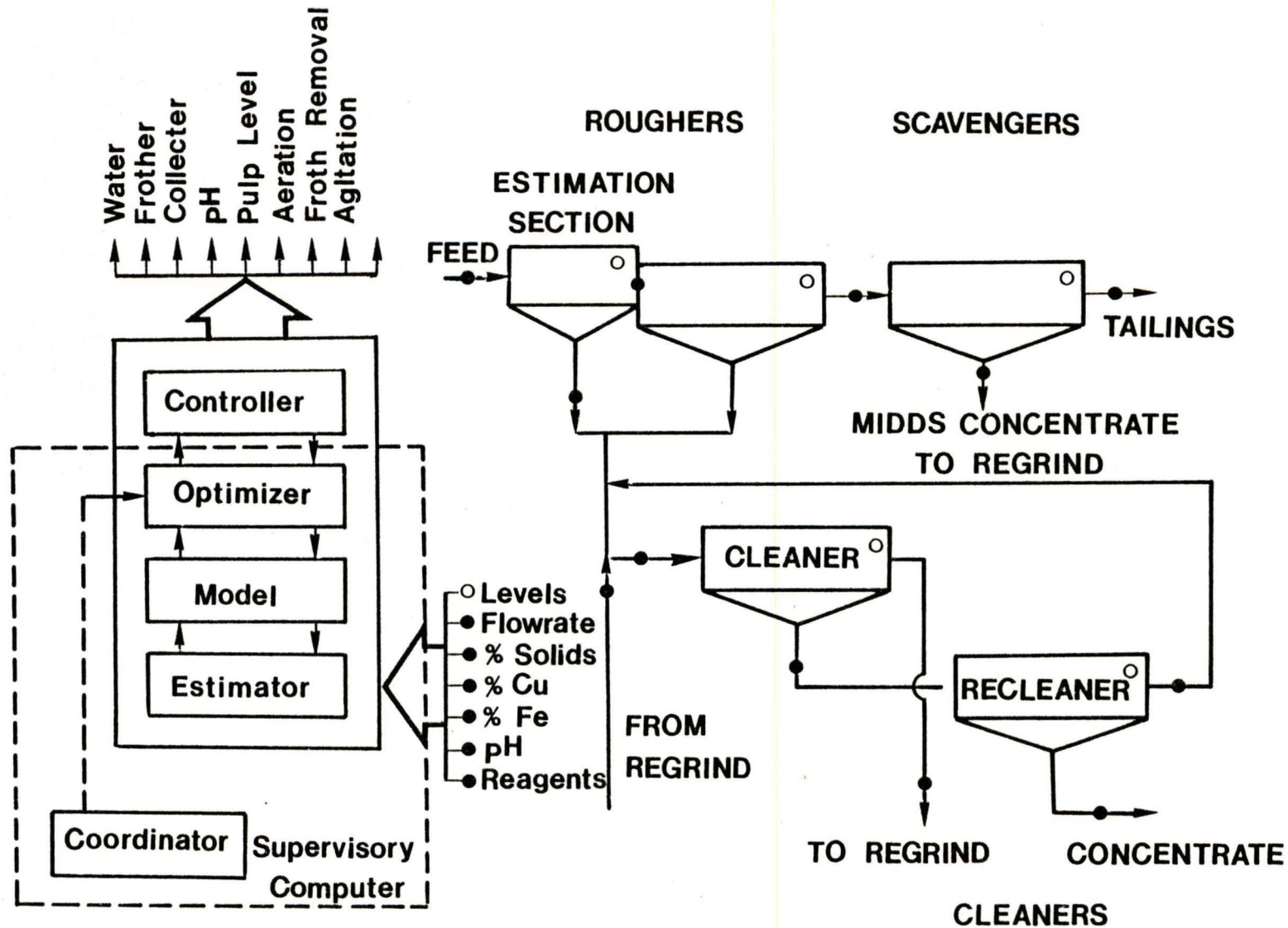


Figure 12. On-Line estimation of ore changes and mass balancing for a copper sulfide flotation circuit.

Control Objectives

A very important factor in the overall design of any control strategy is the selection of an appropriate objective function or performance index. The interactions present in grade-recovery control can be diminished by proper definition of an objective function with the necessary constraints. In practice, every plant will have a different objective which is appropriate for its operation and consistent with management philosophy. In some instances, the control objective may be to maintain a constant and acceptable recovery with other constraints at a constant throughput and may depend on factors like grinding and flotation circuit capacities. Other objectives commonly used in flotation circuits involve maximizing the grade, maximizing throughput, minimizing reagent costs, etc. With the availability of detailed model selection and components, the evaluation of long-term objectives is possible. The model-based control strategy incorporates in a natural way the objective functions to be minimized or maximized in the optimizer block, thus providing the optimal tuning constants for a PI or some other type of controller (see figure 12). In this context, a coordination module provided with new inputs, should the parameters of the form of the objective function change in management or technical policies. Kaggerud (55) reported the application of a phenomenological model and multivariable optimal-control strategy to the primary rougher-flotation bank at the Follidal Verk, Norway, concentrator. However, the strategy is not truly adaptive in that changes in rate constants are not estimated.

Kallioinen (56) describes an optimizing strategy using empirical models obtained for steady-state conditions in the Pyhäsalmi

concentrator in Finland. Because the degree of oxidation of their ore changes abruptly, the need for CuSO_4 is also different for various types of ores, making the control obsolete each time the type of ore changes. After sufficient data is collected, optimization can be performed again and new operating conditions set.

Grade-Recovery Map

It has been determined that the grade-recovery curve obtained in the roughing section determines the total circuit performance in copper sulfide ore flotation (5,54). The flotabilities obtained from the on-line estimator could be used to obtain a grade-recovery map using the flotation model and to define a priori the trajectory of the desired grade-recovery combination, depending on the prevailing plant conditions and parameters. By knowing, a priori, the required froth height, pulp level, aeration rate, frother addition, etc., the setpoints to move in the actual grade-recovery can be defined. This technique allows a form of control-loop decoupling and provides for fast response of the individual controllers.

Figure 13 shows a grade-recovery map obtained using DYNAFLOAT and the parameters obtained from the experimental campaign with a composite of slightly oxidized copper sulfide ore. Several feed rates were exercised for two aeration rates and two pulp levels. Proper limits of the minimum recovery and grade can be set and the desired move will then be exercised by a logical operator computer program which will test for high and low alarms of the critical process variables. This procedure will direct the process to a desired optimal operating constraint. The operator's judgement will finally decide how close to the constraints he wants to stay. According to the actual recovery and grade, the operator

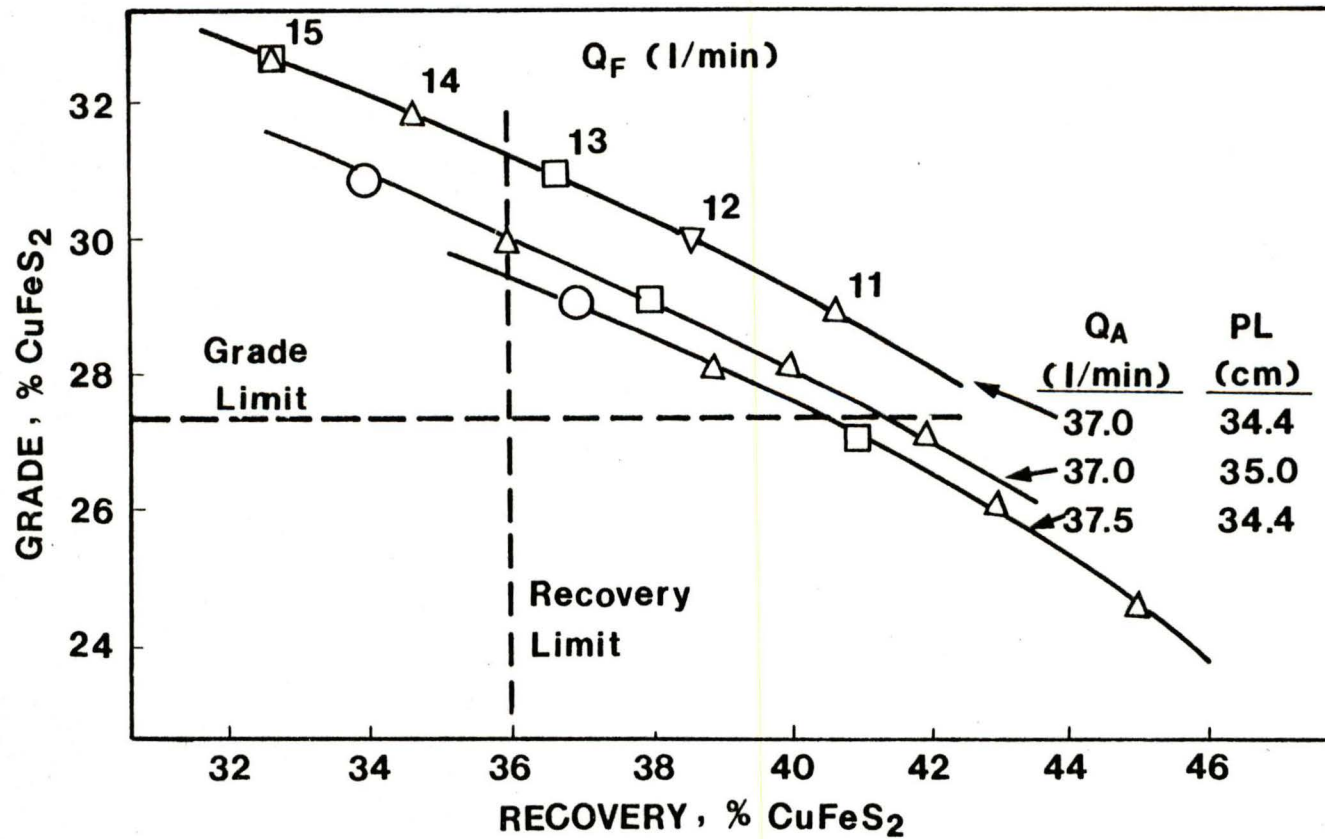


Figure 13. Grade-recovery map provided by the adaptive phenomenological flotation model in the pilot plant.

will move to optimize recovery, to optimize grade, to optimize recovery and grade, or to optimize economic performance.

A close look at figure 13 reveals that in this case a change in pulp level greatly affects the grade and the recovery is only slightly changed. On the other hand, a change in aeration produces an important change in recovery, the grade changing less. All the major interacting mechanisms have been included in the flotation model; thus the sensitivity to a particular mechanism is incorporated in this control method. A good discussion of the common practice in the use of grade-recovery curves in flotation control has been outlined in Thwaites (58).

On-line Adjustment of the Mass Balance

Another area in which the on-line model will prove to be very valuable is in adjusting the mass balance of the overall circuit to provide filtered data from the XRF analyzer. In practice the frequency of invalid information is greatest at the head and tailing streams. Proper weighting and provisions for bad data can be incorporated in the on-line model-filter to provide useful dynamic data in these circumstances (59). Chutskoff and Davies (5) have shown computationally that this concept was possible for the Lake Dufault rougher-scavenger circuit.

*** CONCLUSIONS

A general model framework has been developed wherein principle can be used to represent the behavior of any flotation separation system. The following comments can be made and conclusions can be drawn from the study.

1. The behavior of particles with different mineralogy, namely free valuable, free gangue, and locked, and any number of size intervals can be represented with these model equations.

2. Mechanisms of interphase transfer represented in the kinetic equation include attachment/detachment and entrainment/drainage. In each case the influence of important manipulated variables in the flotation process, such as aeration rate, froth addition, and agitation, on interphase rates are included in the model equations.

3. Particle/bubble and water transport descriptions have been linked to hydrodynamic characteristics in the flotation cell, providing a general framework which includes potential manipulated variables for control.

4. A very important feature of this approach is the hydraulic description contained in the model supported by considerable experimentation in a highly instrumented cell.

5. The comparison of model predictions obtained with the DYNAFLOAT simulator and experimental measurements indicate that the model accurately describes the dynamic response of the separation to a variety of disturbances.

6. Promising control strategies were identified and an important technique for moving through grade-recovery curves from different operating conditions was described based on the predictive capabilities of the flotation model.

7. A simplified flotation model which retains the essential features of the general flotation model seems to provide an appropriate framework for implementing an advanced model-based control philosophy. This advanced control strategy combines the current flotation philosophy of sulfide ores with the capabilities of an on-line estimator.

8. The application of this on-line estimator can be implemented in any operation with adequate instrumentation and computer facilities.

Future efforts should include the actual testing of control strategies and comparison of classical feedback strategies with advanced model-based strategies. A more detailed water model including a complete microscopic description of the froth should probably be developed and included in the overall model equations.

REFERENCES

1. Herbst, J. A., and Bascur, O. A. Mineral-Processing Control in the 1980s -- Realities and Dreams. in J. A. Herbst (ed.), Control 84, SME of AIME, Colorado, 1984, pp 197-215.
2. Bascur, O. A. Modeling and Computer Control of a Flotation Cell. Ph.D. Dissertation, University of Utah, Salt Lake City, Utah (University Microfilms International, Ann Arbor), December, 1982.
3. Reid, K. J., et al., A Survey of Material Balance Computer Packages in the Mineral Processing Industry. 17th APCOM Conference, Proceedings, SME of AIME, New York, 1982.
4. Olsen, T. O., and Henriksen, R. An Innovative Approach to Parameter Estimation in Flotation Processes. in Rajbman (ed.), Identification and System Parameter Estimation, North-Holland Publishing Co., 1978, pp. 1223-1238.
5. Chutskoff, L., and Davies, M. S. Dynamic Modelling and Estimation and Mineral Flotation Circuit Performance. Canadian Metallurgical Quarterly, 19 (1981), 389-393.
6. Niemi, A. J. A Study of the Dynamic and Control Properties of Industrial Flotation Processes. Acta Politechnica Scandinavica, Chemistry Metallurgy Series, No. 48, 1966, pp. 1-111.
7. Niemi, A. J., Maijanen, J., and Niktila, M. T. Singular Optimal Feedforward Control of Flotation. Proceedings of IFAC/FORS Symposium on

Optimization Methods -- Applied Aspects, Varna, Bulgaria, 1974, pp. 277-283.

8. Sadler, L. Y., III. Dynamic Response of the Continuous Mechanical Froth Flotation Cell. Transactions, SME/AIME, v. 254, 1973, pp. 336-343.

9. Greaves, M., and Allan, B. W. Steady-State and Dynamic Characteristic of Flotation in a Single Cell. Transactions, Institution Chemical Engineering, v. 52, 1974, pp. 136-148.

10. Mika, T. S., and Fuerstenau, D. W. A Microscopic Model of the Flotation Process. 8th International Mineral Processing Congress, v. 2, Mechanobr, Leningrad, 1969, pp. 246-269.

11. Lynch, A. J., Johnson, N. W., Manlapig, E. V., and Thorne, C. G. Mineral and Coal Flotation Circuits. Developments in Mineral Processing, Fuerstenau, D. W., advisory editor, v. 3, Elsevier Scientific Publishing Company, 1981.

12. Mehotra, S. P., and Saxena, A. K. Effect of Process Variables on the Residence Time Distribution of Solid in a Continuously Operated Flotation Cell. International Journal of Mineral Processing, v. 4, 1983, pp. 255-277.

13. Moys, M. H. A Study of a Plug-Flow Model for Flotation Froth Behavior, Int. J. Miner. Processing, v. 5, 1978, 21-38.

14. Harris, C. C. Multiphase Models of Flotation Machine Behaviour. Int. J. of Miner. Processing, v. 5, 1978, pp. 107-129.

15. Thorne, G. F. The Behaviour of Lead/Zinc Ores in Industrial Flotation Circuits with Reference to Simulations and Control. Ph.D. Thesis, University of Queensland, Australia, 1975.

16. Kaase, L. Multistage Froth Model for Flotation. M.S. Thesis, University of Utah, Salt Lake City, Utah, in preparation.

17. Flint, L. R. A Mechanistic Approach to Flotation Kinetics. Transactions, Institution of Mining and Metallurgy, v. 83, 1974, pp. C90-C95

18. Randolph, A. D., and Larson, M. A. Theory of Particulate Processes. Academic Press, 1971.

19. Herbst, J. A. An Approach to the Modeling of Rate Processes in Multiparticle Systems. Chapter 2 in Rate Processes in Extractive Metallurgy, H. Y. Sohn and M. E. Wadsworth, eds., Plenum Press, New York, 1979.

20. Laskowski, J. Particle-Bubble Attachment in Flotation. Minerals Science and Engineering, v. 6, no. 4, October 1974, pp. 223-235.

21. Jameson, G. J., Nam, S., and Moo Young, M. Physical Factors Affecting Recovery Rates in Flotation. Minerals Science and Engineering, v. 9, no. 3, July 1977, pp. 103-118.

22. Woodburn, E. T., King, R. P., and Colburn, R. P. The Effect of Particle Size Distribution and the Performance of a Phosphate Flotation Process. Metallurgical Transactions, v. 2, 1971, pp. 3163-3174.

23. Schubert, H., and Bischofberger, C. On the Optimization of Hydrodynamics in Flotation Processes. Mineral Processing, Thirteenth Int. Miner. Processing Congress, Warsaw, June 4-9, 1979, Laskowski, J., ed., v. 2, Elsevier Scientific Publishing Company, New York, 1981, pp. 1261-1287.

24. Abrahamson, J. Collision Rates of Small Particles in a Vigorously Turbulent Fluid. Chemical Engineering Science, v. 30, 1975, pp. 1371-1379.

25. Calderbank, P. H. Physical Rate Processes in Industrial Fermentation, Part 1. Transactions, Institution Chemical Engineers, v. 36, 1959, pp.443-463.
26. Schultze, H. J. New Theoretical and Experimental Investigations on Stability on Bubble/Particle Aggregates in Flotation: A Theory on the Upper Particle Size of Floatability. Int. J. of Miner. Processing, v. 4, 1977, pp. 241-259.
27. Thomas, D. G. Turbulent Disruption of Floccs in Small Particle Size Suspensions. American Institute of Chemical Engineers J., v. 10, no. 4, July 1964, pp. 517-523.
28. Gaudin, A. M. Flotation. 2nd Ed., McGraw-Hill, New York, 1957, pp. 340-355.
29. Spedden, H. R., and Hannan, W. S., Jr. Attachment of Mineral Particles to Air Bubbles in Flotation. Min. Technology, v. 12, no. 2, 1948, pp. 2354.
30. Bascur, O. A. Modeling and Computer Control of a Flotation Cell. Ph.D. Thesis, University of Utah, Salt Lake City, Utah, August 1982.
31. Woodburn, E. T., Kropeller, H., Greene, J., and Cramer, L. The Utility and Limitations of Mathematical Modeling in the Prediction of the Properties of Flotation Networks. Flotation, Fuerstenau, M. C., ed., A. M. Gaudin, v. 2, AIME, New York, pp. 638-674.
32. Booth, R. B., and Freyberger, W. L. Froths and Frothing Agents. Froth Flotation, Fuerstenau, D. W., ed., AIME, New York, pp. 258-276.
33. Klassen, V. I., and Tikhonov, S. A. On the Mechanical Separation of Slimes Particles During Flotation. Tsvetnye Metally, v. 5, no. 9, 1964, pp. 4-8.

34. Derjaguin, B. V., and Dukhin, S. S. Theory of Flotation of Small and Medium-Size Particles. Transactions, Institution of Min. and Metallurgy, vol. 70, 1960-61, pp. 221-246.
35. Kunii, D., and Levenspiel, O. Fluidization Engineering. John Wiley and Sohn, Inc., New York, 1969.
36. Nagata, S. Mixing Principles and Applications. John Wiley and Sohns, Inc., New York, 1975, pp. 345-351.
37. Harris, C. C. Flotation Machines. Flotation, A M. Gaudin Memorial, v. 2, Fuerstenau, M. C., ed., American Institute of Min., Metallurgical and Petroleum Engineers, New York, NY, 1976, pp. 753-815.
38. Schubert, H. Zur Proze Bestimmenden Rolle der Turbulenz bei Aufbereitungsprozessen-2.Teil. Aufbereitungs Technik, v. 12, 1974, pp. 680-685.
39. Van Landehem, H. Multiphase Reactors: Mass Transfer and Modeling. Chemical Engineering Science, v. 35, 1980, pp. 1912-1949.
40. Levich, V. G. Physicochemical Hydrodynamics. Prentice Hall, Inc., Englewood Cliffs, New Jersey, 1962.
41. Clift, R., Grace, J. R., and Weber, M. E. Bubbles, Drops and Particles, Academic Press, New York, 1980.
42. Barker, I. J. Investigation into the Effects of Froth Height in a Flotation Cell. M.S. Thesis, University of Natal, Durban, South Africa, 1971.
43. Bikerman, J. J. Foams. Springer-Verlag, New York, Heidelberg, Berlin, 1973.
44. Barber, A. D., and Hartland, S. The Collapse of Cellular Foams. Transactions, Institution of Chemical Engineers, v. 53, 1975, pp. 106-111.

45. Harris, C. C., and Raja, A. A Modified Laboratory Flotation Cell. Transactions, American Institute of Mining Engineers, v. 235, 1966, pp. 150-156.
46. Perry, R. H., and Chilton, C. H., eds. Chemical Engineer Handbook. Fifth Ed., McGraw-Hill Kogakusha, Ltd., 1973, Chapter 5, p. 17.
47. Herbst, J. A., and Rajamani, K. Application of Modern Control Theory to Mineral Processing Operations. 12th CMMI Congress, Johannesburg, South Africa, May 1982.
48. Himmelblau, D. M. Applied Nonlinear Programming. McGraw-Hill, New York, 1972.
49. Maybeck, P. S. Stochastic Models, Estimation and Control. V. 2 and 3, Academic Press, New York, New York, 1982.
50. Ray, H. W. Advanced Process Control. McGraw-Hill Book Co., New York, New York, 1981, p. 376.
51. Maybeck, P. S. Stochastic Models, Estimation and Control. V. 1, Academic Press, New York, New York, 1979.
52. Shinskey, F. G. Process Control Systems, Applications, Design, Adjustment. McGraw-Hill Book Co., New York, New York, 1967.
53. Herbst, J. A., and Bascur, O. A. Grade/Recovery Control in Froth Flotation by Joint Manipulation of Aeration and Impeller Speed. Patent disclosure, University of Utah, January 10, 1981.
54. McKee, D. J., Fewings, J. H., Manlapig, E. V., and Lynch, A. J. Computer Control of Chalcopyrite Flotation at Mount Isa Mines Limited. Flotation, M. C. Fuerstenau (ed.), SME of AIME, New York, New York, 1976, pp. 994-1026.

55. Kaggerud, I. Experiences with Optimal Control and Flotation Plants. 4th IFAC Symposium in Automation in Mining, Mineral, and Metal Processing, Finland, 1983, pp. 427-433.
56. Kallioinen, J. O. The Control of Zinc Flotation: Comparison of Two Concentrators. Control 84, Herbst, J. A., ed., SME of AIME, Colorado, 1984, pp. 261-268.
57. Lynch, A. J., Johnson, N. W., Manlapig, E. V., and Thorne, C. G. Mineral and Coal Flotation Circuits, Their Simulation and Control. Elsevier Scientific Publishing Company, 1981, p. 291.
58. Thwaites, P. Continued Development of Copper Flotation Control at the Kidd Creek Concentrator. CIM Bulletin, December 1983.
59. Ramagnoli, J. A. On Data Reconciliation: Constraints Processing and Treatment of Bias. Chemical Engineering Science, v. 38, 1983, pp. 1107-1117.
60. Bascur, O. A. Bi-Dimensional Fluidized Froth Column. Patent Disclosure, University of Utah, January 1981.